Highly Accurate First-Principles Benchmark Data Sets for the Parametrization and Validation of Density Functional and Other Approximate Methods. Derivation of a Robust, Generally Applicable, Double-Hybrid Functional for Thermochemistry and Thermochemical Kinetics†

Amir Karton,‡ Alex Tarnopolsky,‡ Jean-François Lamère,‡ George C. Schatz,§ and Jan M. L. Martin*,§,||

Department of Organic Chemistry, Weizmann Institute of Science, IL-76100 Rechovot, Israel, and Department of Chemistry, Northwestern University, 2145 Sheridan Road, Evanston, Il 60208-3113

Received: February 29, 2008; Revised Manuscript Received: April 23, 2008

We present a number of near-exact, nonrelativistic, Born−Oppenheimer reference data sets for the parametrization of more approximate methods (such as DFT functionals). The data were obtained by means of the W4 ab initio computational thermochemistry protocol, which has a 95% confidence interval well below 1 kJ/mol. Our data sets include W4-08, which are total atomization energies of over 100 small molecules that cover varying degrees of nondynamical correlations, and DBH24-W4, which are W4 theory values for Truhlar's set of 24 representative barrier heights. The usual procedure of comparing calculated DFT values with experimental atomization energies is hampered by comparatively large experimental uncertainties in many experimental values and compounds errors due to deficiencies in the DFT functional with those resulting from neglect of relativity and finite nuclear mass. Comparison with accurate, explicitly nonrelativistic, ab initio data avoids these issues. We then proceed to explore the performance of B2x-PLYP-type double hybrid functionals for atomization energies and barrier heights. We find that the optimum hybrids for hydrogen-transfer reactions, heavy-atoms transfers, nucleophilic substitutions, and unimolecular and recombination reactions are quite different from one another: out of these subsets, the heavy-atom transfer reactions are by far the most sensitive to the percentages of Hartree−Fock-type exchange *y* and MP2-type correlation *x* in an (*x*, *y*) double hybrid. The (42,72) hybrid B2K-PLYP, as reported in a preliminary communication, represents the best compromise between thermochemistry and hydrogen-transfer barriers, while also yielding excellent performance for nucleophilic substitutions. By optimizing for best overall performance on both thermochemistry and the DBH24-W4 data set, however, we find a new (36,65) hybrid which we term B2GP-PLYP. At a slight expense in performance for hydrogen-transfer barrier heights and nucleophilic substitutions, we obtain substantially better performance for the other reaction types. Although both B2K-PLYP and B2GP-PLYP are capable of 2 kcal/mol quality thermochemistry, B2GP-PLYP appears to be the more robust toward nondynamical correlation and strongly polar character. We additionally find that double-hybrid functionals display excellent performance for such problems as hydrogen bonding, prototype late transition metal reactions, pericyclic reactions, prototype cumulene−polyacetylene system, and weak interactions.

I. Introduction

Very recently, we published a preliminary communication[1] showing that a double-hybrid functional that we denoted B2K-PLYP yields excellent performance (approaching that of compound ab initio thermochemistry methods)[2,3] for all of the following: (a) main-group thermochemistry, (b) main-group barrier heights, and (c) barrier heights for late transition metal reactions.

The term "double hybrid" was originally coined by Truhlar[4] for multistep methods involving both DFT and ab initio steps but has become associated with the name of Grimme,[5,6] who proposed the original functional class of which B2K-PLYP is a special case.

Formally, B2K-PLYP and Grimme's earlier B2-PLYP[5] and mPW2-PLYP[6] are fifth-rung functionals on the Jacob's Ladder outlined by Perdew.[7] In Perdew's metaphor, ground level would be Hartree product SCF (null exchange, null correlation) and Heaven the exact exchange-correlation functional, with each successive rung of the ladder introducing an additional piece of information. The first rung employs just the density and corresponds to the local spin density approximation. The reduced density gradient is introduced on the second rung, which is occupied by the various GGAs (generalized gradient approximations) such as BLYP[8,9] and PBE.[10] Higher-order local derivatives (or related variables such as the kinetic energy density) enter on rung three, occupied by the various meta-GGAs such as TPSS[60] and M06L.[15] At the fourth rung, the occupied orbitals are introduced: this leads to hybrid GGA functionals such as PBE0,[11] B3PW91,[12,13] and the very popular B3LYP[13] and hybrid meta-GGAs such as BMK[14] and the M06 family.[15–18] Finally, the fifth rung is climbed by additionally introducing the virtual orbitals: double-hybrid functionals

† Part of the "Sason S. Shaik Festschrift".

* Corresponding Author. E-mail: gershom@weizmann.ac.il.
‡ Weizmann Institute of Science.
§ Northwestern University.
|| On sabbatical from Weizmann Institute of Science.

10.1021/jp801805p CCC: $40.75
Published on Web 08/20/2008

constitute one special case thereof. (We note that an extensive review of orbital-dependent functionals has appeared very recently.)[19]

Operationally, a double-hybrid calculation consists of the following steps. First, the Kohn−Sham equations are solved self-consistently for a given hybrid GGA or meta-GGA functional with $100c_1$ percent exact exchange and the correlation functional damped by a factor $1 - c_2$. Subsequently, the MP2 (second-order perturbation theory) correlation energy is calculated in the space of the converged Kohn−Sham orbitals (effectively making it second-order Görling-Levy perturbation theory).[20] (The f_{ia} type elements that would, strictly speaking, be required for a reference wave function that does not satisfy the Brillouin theorem are neglected both by Grimme and in our work.) Finally, the total energy is obtained as

$$E_{xc} = (1 - c_1)E_{x,GGA} + c_1E_{x,HF} + (1 - c_2)E_{c,GGA} + c_2E_2 \quad (1)$$

where $E_{x,GGA}$ and $E_{c,GGA}$ represent the exchange and correlation parts of the underlying DFT functional, $E_{x,HF}$ and E_2 are the Hartree−Fock type exchange energy and MP2 correlation energy, respectively, in the basis of the converged Kohn−Sham orbitals, and c_1 and c_2 are empirical mixing coefficients. The specific $E_{c,GGA}$ considered by Grimme was Lee−Yang−Parr (LYP),[9] combined with the Becke88 exchange functional[8] into B2-PLYP[5] (with $c_1 = 0.53$ and $c_2 = 0.27$) and with modified Perdew−Wang (mPW) exchange[21] into mPW2-PLYP[6] (with $c_1 = 0.55$ and $c_2 = 0.25$). In the remainder of this article, we will use the notation (x,y) for a double hybrid with y% Hartree−Fock type exchange and x% MP2-type correlation: B2-PLYP thus becomes a (27,53) and mPW2-PLYP a (25,55) double hybrid, with B2K-PLYP being a (42,72) double hybrid.

Energy calculations of this type can in fact be carried out, albeit with some nonstandard input decks, by using unmodified versions of certain popular quantum chemical codes such as Gaussian 03.[22] Very recently, Neese et al.[23] implemented analytical first derivatives for such methods in the freeware quantum chemistry program system ORCA.[24]

With conventional MP2 codes, the MP2 step represents a considerable additional expense, which would seem to obviate one of the main advantages of DFT over wave function ab initio methods. However, with the RI-MP2 approximation,[25] this issue can basically be eliminated at very little loss in accuracy.

A physical rationale for these functionals[26] may lie in the fact that although typical DFT correlation functionals will be superior to MP2 in the description of short-range correlation, MP2 is very well suited for the description of long-range correlation, and a marriage of convenience between the two correlation methods may thus have a fighting chance of handling both types of correlation.

The Martin group is heavily involved in organic (e.g., ref 27) and organometallic (e.g., refs 28–31) mechanistic chemistry. Much of its research involves multiple competing reaction pathways with intermediate energies and reaction barrier heights that are within a few kcal/mol of each other. The Schatz group, for its part, has a long-standing interest in heavy-atom transfer (HAT) reactions of relevance to hyperthermal reactions (e.g., refs 32 and 33).

As such, we are highly interested in a functional that can handle all of the following with 1−2 kcal/mol accuracy: (1) main-group thermochemistry, (2) main-group barrier heights, and (3) reactions at late transition metal centers. As we found in a recent validation study,[34] none of the currently available hybrid GGAs and meta-GGAs are able to pass more than two out of these three litmus tests.

We already showed in our preliminary communication[1] that double hybrids are capable of passing all three tests. Specifically, we showed that thermochemical performance of double hybrids is nearly constant in two-dimensional (%MP2,%HF) space along a narrow canal (the location of which along the MP2 axis displays some basis-set dependence), whereas performance for hydrogen-transfer barrier heights displays a more conventional basin. At the point where basin and canal approach each other, (42,72), a double hybrid (B2K-PLYP) can be found that offers excellent performance for both thermochemistry and kinetics.

A number of questions remained unanswered and will be addressed in the present paper. First, it is not a priori clear that different reaction classes, such as HATs, are best served by a kinetics double hybrid optimized for hydrogen-transfer reactions. Second, the discrepancies between calculated and experimental atomization energies, for instance, are no longer on grossly different scales from various effects included in the experimental data but not in the computational model, such as relativity, deviations from the Born−Oppenheimer approximation, and anharmonic zero-point vibration corrections.

As a byproduct of the Martin group's activity in high-accuracy computational thermochemistry, however,[35–42] we have accumulated a fairly large database of thermochemical data at the W4 theory[38] level. Not only does the 95% confidence interval of 0.16 kcal/mol of W4 data[38] surpass all but the very best experimental data (which are available for a very limited number of systems), but clamped-nuclei, zero-point exclusive (a.k.a., bottom of the well) components of these data are trivially isolated. In the present work, we will augment the thermochemistry data with additional calculations to obtain a reliable thermochemical benchmark set, as well as present an entirely new such data set for barrier heights. We will also show that these sets offer a much more detailed and controllable picture than conventional methods.

Furthermore, we will show that different classes of reactions do indeed have different requirements but that best performance overall is mostly driven by HAT reactions, as well as thermochemistry. We will present a new double hybrid, B2GP-PLYP (GP for general purpose), which has all the advantages of B2K-PLYP but more balanced performance for different reaction classes and displays considerably greater robustness.

Finally, we will obtain high-level ab initio reference data for a number of problems where DFT traditionally yields the wrong answer and show that double hybrids handle these with some aplomb.

II. Computational Methods

All electronic structure calculations reported here were carried out on the Martin group Linux cluster at Weizmann. Post-CCSD(T) ab initio calculations were performed by means of the MRCC general coupled cluster program by Kállay[43] interfaced to the Austin−Mainz−Budapest version of ACES II.[44] (The latter was also used for the diagonal Born−Oppenheimer corrections required in W4 theory.) Large basis-set CCSD and CCSD(T) calculations were run by using MOLPRO 2006.1.[45] All density functional calculations (including the double hybrids) were carried out by using the Weizmann locally modified version of the Gaussian 03 electronic structure program.[22]

The computational protocol for W4 theory has been described in great detail elsewhere[38] and will not be repeated here. Suffice to say that the W4 final energy consists of the following components: (a) SCF, (b) valence CCSD correlation, (c) valence

(T) correlation, (d) higher-order connected triples T_3-(T), (e) connected quadruples T_4, (f) connected quintuples T_5, (g) CCSD(T) inner-shell correlation, (h) Douglas−Kroll CCSD(T) scalar relativistics, (i) first-order spin−orbit coupling, and (j) diagonal Born−Oppenheimer correction (DBOC). We will report both complete W4 values and nonrelativistic, clamped-nuclei, W4 values (i.e., exclusive of scalar relativistics, spin−orbit, and DBOC). The former are of thermochemical interest, the latter enable direct apples-to-apples comparisons of the DFT data.

As byproducts of the W4 calculation, additional data at lower levels of theory are obtained, such as W2.2, W3.2, and W4lite.[38] W1 values reported in the present paper were obtained by using the implementation in Gaussian 03.[22] This implementation, unlike the original paper,[35] uses unrestricted Hartree−Fock reference wave functions for open-shell systems and is inclusive of a spin-contamination correction proposed in ref 46. Various other multistep ab initio thermochemistry protocols, such as G2 theory,[47] G3 theory,[48] CBS-QB3,[49] G3X theory,[50] and G4 theory,[51] were likewise run either directly by using Gaussian or (in the cases of G3X and G4) by using simple drivers for Gaussian.

The basis sets used in the DFT calculations belong to the polarization-consistent family of Jensen.[52–56] We primarily considered two basis sets: aug-pc2 (which is of triple-ζ spdf + diffuse quality and quite close to the Kohn−Sham basis-set limit for DFT calculations) and aug-pc3 (which is of quadruple-to-quintuple-ζ spdfg + diffuse quality and was required for basis-set convergence in the double-hybrid calculations). As required for the proper treatment of second-row atoms in high oxidation states,[57] high-exponent d functions were added. In order to verify convergence, we also carried out some calculations using the even larger aug-pc4 basis set.

In the comparisons, we considered a number of other exchange-correlation functionals, such as B3LYP,[13] BMK,[14] PBE0,[11] B1B95,[58] B97−1[59] TPSSKCIS,[60–62] BB1K,[63] mPW1B95,[64] PW6B95,[65] and PWB6K,[65] as well as the very recent M06 (Minnesota-06) family of functionals.[15–17]

III. Results and Discussion: Ab Initio Reference Data Sets

A. General Remarks. Most of the data discussed below are obtained at the W4 level.[38] By comparison with ATcT (active thermochemical tables)[66] data for a number of key species, we were able to establish an rms deviation (rmsd) from ATcT of only 0.08 kcal/mol, which implies an approximate 95% confidence interval of 0.16 kcal/mol. This is at least an order of magnitude less than the intrinsic errors of the methods being discussed here.

In fact, for the larger species, it appears[39] that the main factor limiting accuracy of the ab initio calculations is not the solution of the electronic Schrödinger equation but that of the nuclear Schrödinger equation (specifically, the zero-point vibrational energy), especially for nonrigid systems. Because for our present purpose, however, we are explicitly interested in clamped-nuclei data, the zero-point vibrational energies become a nonissue.

B. DBH24-W4. The DBH24 (24 diverse barrier heights) was assembled by Zheng, Zhao, and Truhlar (ZZT)[67] as a small, but representative, data set of barrier heights for assessing the performance of computational chemistry methods for thermochemical kinetics. Their own reference data were primarily obtained at the W1 level[35] from QCISD/MG3[68] reference geometries.

The DBH24 set consists of four subsets of six barriers each for HAT, nucleophilic substitution (SN2), hydrogen transfer (Hxfer), and unimolecular and recombination (UAR) reactions, all selected from much larger data sets[69] of 38 Hxfers (HTBH38) and 38 nonHxfer (NHTBH38).

In our own calculations, we have used their geometries without further reoptimization.[67] Our results, compared with those from ref 67, are given in Table 1. We carried out W3.2 calculations for all reactions and W4 for a subset.

In most cases, the discrepancies between our best data and those of ZZT are very small, confirming that W1 is indeed generally a reliable method for generating this type of benchmark data. The exception is represented by the HATs, where discrepancies on the order of up to 1 kcal/mol are seen. This is consistent with earlier observations[1,67,69] that the HATs are by far the hardest subclass to reproduce by quantum chemical methods (see also below).

C. W4-08. This set, compiled in Table 2, represents partly a compilation from earlier published data by the Martin group[38–42] and partly new data. We earlier showed[38] that %[(T)], the percentage of the total atomization energy accounted for by connected triple excitations, is a simple and reliable gauge of nondynamical correlation effects: the W4-08 set spans a wide gamut from systems dominated by dynamical correlation (such as H_2O and CH_4) to systems with pathological nondynamical correlation (O_3, C_2, and BN) and all shades in between. We even included the Be_2 dimer, the potential curve of which is actually repulsive at the CCSD level.

Our earlier calculated data were also quite diverse in terms of ionic versus covalent bonding character and included a few species with strong inner polarization[72] such as SO_3.[73] These data were however somewhat thin on open-shell species, and therefore, many of the new species in Table 2 are radicals. Many of these are related to the ongoing work[71] of a IUPAC task group on radical thermochemistry that one of us (J.M.L.M.) is a member of. Others relate to a forthcoming paper[74] on halogen oxides and peroxides that is presently in preparation—we have included them here because particularly the peroxide species are notoriously difficult for conventional electronic structure methods.[75]

All data provided in Table 2 were obtained at least at the W4 level, some at even higher levels, such as W4.2,[38] W4.3,[38] and W4.4.[40]

D. Miscellaneous. It was noticed some time ago[77,78] that DFT methods have considerable difficulties reproducing the subtle equilibrium between cumulenic and acetylenic structures. The smallest prototype for this is of course the equilibrium between the C_3H_4 isomers allene and propyne, where we have thrown in cyclopropene for good measure. At the W4.2 level, our computed (nonrelativistic, clamped-nuclei, zero-point exclusive) total atomization energies in kcal/mol are 705.56 for propyne, 704.06 for allene, and 682.00 for cyclopropene. This results in isomerization energies, again in kcal/mol, of 1.50 for propyne to allene, 22.06 for allene to cyclopropene, and 23.56 for propyne to cyclopropene. The CCCBDB[76] TAEs at 0 K are 670.7 ± 0.4, 669.1 ± 0.4, and 648.2 ± 0.8 kcal/mol for propyne, allene, and cyclopropene, respectively. By including scalar relativistic, first-order spin orbit coupling, DBOC, and anharmonic (B3LYP/pc-2) ZPVE corrections, we obtain at the W4.2 level (in kcal/mol) 670.51 ± 0.14 for propyne, 669.33 ± 0.14 for allene, and 646.73 ± 0.14 for cyclopropene. Our W4.2 TAEs for propyne and allene are +0.2 and −0.2 kcal/mol away from experiment, respectively, but for cyclopropene, the W4.2 value is 1.5 kcal/mol lower than that the experimental value. The relativistic (DBOC-inclusive) W4.2 isomerization energies at 0 K are 1.18 for propyne to allene, 22.59 for allene to

TABLE 1: W4 and W3.2 Relative Barrier Heights for the DBH24 Dataset (kcal/mol)

	TAE $_e$ [a]	TAE $_0$ [b]	TAE $_0$ [c]	Truhlar [d]
		Forward		
		HATBH6		
$H + N_2O \rightarrow OH + N_2$ [e]	17.19	17.23	17.13	18.14
$H + ClH \rightarrow HCl + H$ [e]	17.60	17.47	17.47	18.00
$CH_3 + FCl \rightarrow CH_3F + Cl$ [f]	6.90	6.77	6.75	7.43
		NSBH6		
$Cl^- \cdot\cdot\cdot CH_3Cl \rightarrow ClCH_3 \cdot\cdot\cdot Cl^-$ [f]	13.53	13.42	13.41	13.61
$F^- \cdot\cdot\cdot CH3Cl \rightarrow FCH_3 \cdot\cdot\cdot Cl^-$ [f]	3.50	3.45	3.44	2.89
$OH^- + CH_3F \rightarrow HOCH_3 + F^-$ [f]	−2.40	−2.44	−2.44	−2.78
		UABH6		
$H + N_2 \rightarrow HN_2$ [e]	14.32	14.52	14.36	14.69
$H + C_2H_4 \rightarrow C_2H_5$ [e]	1.83	1.84	1.83	1.72
$HCN \rightarrow HNC$ [e]	48.14	48.10	48.07	48.16
		HTBH6		
$OH + CH_4 \rightarrow CH_3 + H_2O$ [e]	6.13	6.54	6.35	6.7
$H + OH \rightarrow O + H_2$ [e]	10.65	10.74	10.77	10.7
$H + H_2S \rightarrow H_2 + HS$ [e]	3.77	3.76	3.69	3.6
		Reverse		
		HATBH6		
$H + N_2O \rightarrow OH + N_2$ [e]	82.14	82.56	82.47	83.22
$H + ClH \rightarrow HCl + H$ [e]	17.60	17.47	17.47	18.00
$CH_3 + FCl \rightarrow CH_3F + Cl$ [f]	59.33	60.04	60.00	61.01
		NSBH6		
$Cl^- \cdot\cdot\cdot CH_3Cl \rightarrow ClCH_3 \cdot\cdot\cdot Cl^-$ [f]	13.53	13.42	13.41	13.61
$F^- \cdot\cdot\cdot CH3Cl \rightarrow FCH_3 \cdot\cdot\cdot Cl^-$ [f]	29.53	29.42	29.42	29.62
$OH^- + CH_3F \rightarrow HOCH_3 + F^-$ [f]	17.77	17.69	17.66	17.33
		UABH6		
$H + N_2 \rightarrow HN_2$ [e]	10.70	10.73	10.61	10.72
$H + C_2H_4 \rightarrow C_2H_5$ [e]	41.88	41.83	41.84	41.75
$HCN \rightarrow HNC$ [e]	32.92	32.86	32.82	33.11
		HTBH6		
$OH + CH_4 \rightarrow CH_3 + H_2O$ [e]	19.36	19.51	19.26	19.6
$H + OH \rightarrow O + H_2$ [e]	12.90	13.18	13.17	13.1
$H + H_2S \rightarrow H_2 + HS$ [e]	17.09	17.83	17.75	17.3

[a] W*n* Zero-point exclusive, nonrelativistic, clamped-nuclei TAEs for testing/parametrization of DFT functionals. [b] W*n* Zero-point exclusive, relativistic, first-order spin orbit TAEs with DBOC (for comparison with experiment ZPVE should be included as well). [c] W*n* Zero-point exclusive, relativistic, clamped-nuclei, first-order spin orbit TAEs for comparison with Truhlar's values. [d] Table 2 of ref 67. [e] From W4 theory. [f] From W3.2 theory.

cyclopropene, and 23.78 for propyne to cyclopropene and are in qualitative agreement with the experimental isomerization energies.

In addition, we have obtained benchmark data for some pseudohypervalent species, such as PF_5 and SF_6, as well as for some other species with strong inner polarization, such as $HClO_3$, $HClO_4$, and SiF_4. As these species are presently beyond the reach of full W4 calculations for various technical reasons, these data are of somewhat lower quality than those in the W4-08 set and will consider them separately. They can be found in Table 3.

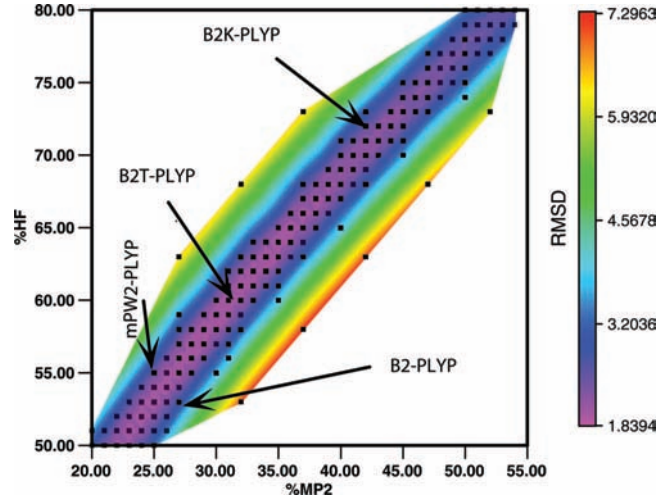

Figure 1. rmsd (kcal/mol) for the W3 atomization energies data set of double-hybrid B2-PLYP forms as a function of the percentages of MP2-type correlation (abscissa) and HF-type exchange (ordinate). Black dots indicate actual data points. The aug-pc3 basis set was used throughout.

E. Existing Reference Data Sets. Additional performance assessments for Hxfer and non-Hxfer barrier heights were carried out against the HTBH38 and NHTBH38 data sets of the Truhlar group.[69] Performance for late transition metal barrier heights was assessed by using the W1-level data of Quintal et al.[34] for a number of prototype reactions at Pd(0). Furthermore, performance for weak interactions was assessed against the benchmark set of Zhao and Truhlar[80] and its subsets of six hydrogen bonds (HB6), seven charge-transfer complexes (CT7), six dipole-bound complexes (DI6), and nine van der Waals complexes (WI9). Among these, hydrogen bonds were subjected to somewhat closer scrutiny against the very recent data set of Boese et al.,[70] which contains 16 hydrogen-bonded complexes, 11 of which are neutral, and five are cationic or anionic. These latter data were obtained by using W2 theory at CCSD(T)/A′VQZ reference geometries. In addition, we considered the S22 weak interactions reference data of Hobza and co-workers,[81] which includes systems as large as nucleic acid dimers. For all these data sets, the published reference geometries were employed unchanged.

IV. Results and Discussion: Performance of Double-Hybrid Functionals

A. Thermochemistry. In our preliminary communication,[1] we noted that the rmsd surface for total atomization energies as a function of the twin variables (%MP2,%HF) exhibits a narrow canal or straits along which performance is optimal rather than a clear minimum. A contour plot of the B2x-PLYP/aug-pc3+d rmsd surface for the W3 set of molecules[37] can be seen in Figure 1.

As noted in ref 1, the locus of the straits is somewhat basis-set dependent, because smaller basis sets will lead to exaggerated admixtures of MP2-like correlation in order to compensate. (One price the user pays for inclusion of MP2-like correlation is that the method partially inherits the slow basis-set convergence of

TABLE 2: W4-08 Dataset[g] (W*n* Total Atomization Energies, in kcal/mol)

W4				W4.4				W4.3				W4.2			
	TAE_e[a]	TAE_e[b]	TAE_0[c]		TAE_e[a]	TAE_e[b]	TAE_0[c]		TAE_e[a]	TAE_e[b]	TAE_0[c]		TAE_e[a]	TAE_e[b]	TAE_0[c]
B_2H_6	607.02	606.83	567.53	H_2	109.49	109.51	103.28	Be_2	2.67	2.66	2.29	BN[d]	105.82	105.73	103.56
BHF_2	410.97	409.75	398.73	OH	107.21	107.05	101.76	B_2	67.46	67.35	65.85	CF	132.72	132.21	130.35
BF_3[h]	470.97	496.75	461.32	HF	141.64	141.12	135.27	BH	84.99	84.84	81.49	BeF_2	309.10	307.91	303.64
C_2H_6	713.08	712.67	666.28	H_2O	232.97	232.58	219.32	BH_3	281.29	281.17	264.80	CH_2C	359.93	359.63	345.10
H_2CN	343.75	343.45		CH	84.22	84.03	79.99	BN[e]	105.24	105.05	102.62	CH_2=CH	446.08	445.68	423.06
NCCN[l]	502.04	501.35	491.50	CH_2	190.74	190.53	179.86	BF	182.52	181.95	179.96	C_2H_4	564.10	563.71	532.11
CH_2NH_2	482.28	481.87	451.03	CH_3[j]	307.87	307.63	289.08	NH	83.10	82.98	78.34	CH_2NH	439.44	439.10	414.41
CH_3NH	474.63	474.24	444.22	CH_4[j]	420.42	420.20	392.46	NH_2	182.59	182.43	170.58	HC=O	279.42	278.71	270.66
CH_3NH_2	582.30	581.91	542.22	C_2H	266.16	265.73	257.04	HCN	313.42	313.19	303.21	H_2CO	374.66	374.04	357.51
CF_2	258.78	257.63	253.26	C_2H_2	405.52	405.16	388.70	HOF	158.65	157.90	149.32	CO_2	390.14	389.18	381.94
N_2H	224.86	224.58		NH_3[j]	298.02	297.86	276.53	AlH[j]	73.57	73.22	70.83	HNO	205.89	205.34	196.78
N_2H_2	296.53	296.25	278.68	C_2	147.02	146.71	144.06	AlH_3[j]	213.17	212.52	200.92	NO_2	227.88	227.01	221.61
N_2H_4	438.28	437.94	404.73	N_2	228.48	228.36	225.00	AlF[j]	163.78	162.90	161.76	N_2O	270.85	270.21	263.43
FO_2	134.72	133.71	130.15	CO	259.73	259.26	256.15	AlCl	122.62	121.32	120.64	O_3	147.43	146.48	142.34
F_2O_2[h]	152.37	150.83	145.83	CN	181.35	181.13	178.18	SiH	73.92	73.54	70.65	HO_2	175.53	174.82	165.97
AlF_3[h]	430.97	428.32	423.47	NO	152.75	152.51	149.80	SiH_4	324.95	323.85	304.16	H_2O_2	269.09	268.39	252.08
Si_2H_6[h]	535.89	533.72	503.09	O_2	120.82	120.21	117.96	SiO	193.05	192.14	190.37	F_2O	93.78	92.68	89.43
P_4[h]	290.58	289.87	285.96	OF	53.08	52.67	51.17	SiF[j]	142.71	141.84	140.62	HOCl	166.23	164.91	156.73
SO_2	260.62	258.80	254.42	F_2	39.04	38.25	36.95	CS	172.22	171.42	169.59	S_2H	165.13	163.51	157.68
SO_3[h]	346.94	343.91	336.12	PH_3[j]	242.27	241.80	227.36								
OCS	335.75	334.37	328.65	HS	87.73	87.52	83.71								
CS_2	280.78	278.97	274.67	H_2S[j]	183.91	182.98	173.58								
S_2O	208.78	206.77	203.57	HCl[j]	107.50	106.44	102.20								
S_3	168.36	166.13	163.96	SO[j]	126.47	125.34	123.70								
S_4[f,h]	234.35	231.44	228.15	ClO	65.45	64.62	63.40								
$BeCl_2$	225.27	223.09	220.20	ClF[j]	62.80	61.40	60.28								
CCl_2	177.36	175.33	172.72	P_2	117.59	117.33	116.21								
$AlCl_3$[h]	312.65	308.65	305.59	S_2[j]	104.25	102.81	101.78								
ClCN	285.45	284.12	278.79	Cl_2[j]	59.75	57.87	57.07								
OClO	128.12	125.99	122.33												
ClOO	126.39	124.96	121.89												
Cl_2O	101.46	99.31	96.93												

[a] Zero-point exclusive, nonrelativistic, clamped-nuclei total atomization energies. [b] Zero-point exclusive, relativistic, DBOC total atomization energies. [c] Total atomization energies at 0 K. [d] $^3\Pi$ state, $r = 1.3302$Å. [e] $^1\Sigma^+$ state, $r = 1.2830$Å. [f] C_{2v} symmetry. [g] ZPVEs: C_2H_2, CH_3, CO_2, N_2O, O_3, NO_2, CF, ClF, CS, HOCl, PH_3, SO_2, OCS, ClCN, C_2H_4, H_2CO, and HNO from ref 38; C_2H_6 from ref 39; H_2, OH, H_2O, C_2H_2, CH_4, CH, CO, F_2, HF, N_2, NH_3, NO, O_2, Cl_2, HCl, H_2S, SO, S_2, CN, B_2, and C_2 from ref 40; Be_2, BeF_2, $BeCl_2$, BH, BF, BH_3, BHF_2, B_2H_6, BF_3, AlH, AlH_3, AlF, AlF_3, AlCl, $AlCl_3$, SiH, SiF, SiH_4, and Si_2H_6 from ref 41; P_2 and P_4 from ref 42; OClO, ClOO, Cl_2O, OF, ClO, HOF, F_2O, F_2O_2, FO_2, HO_2, and H_2O_2 from ref ; H_2CN, NCCN, CH_2NH_2, CH_3NH, CH_3NH_2, CF_2, N_2H, N_2H_2, N_2H_4, SO_3, CS_2, S_2O, S_3, S_4, CCl_2, CH_2, C_2H, HS, NH, NH_2, HCN, SiO, CH_2C, CH_2CH, CH_2NH, HCO, and S_2H from this work, see Supporting Information. [h] For BF_3, F_2O_2, AlF_3, Si_2H_6, P_4, SO_3, S_4, and $AlCl_3$, $\hat{T}_5 \approx$ CCSDTQ(5)$_\Lambda$ − CCSDTQ = 0.02, 0.27, 0.04, 0.00, 0.13, 0.21, 0.30, and −0.01 kcal/mol, respectively. [l] $\hat{T}_5 \approx$ CCSDTQ(5) − CCSDTQ = 0.24 kcal/mol. [j] $\hat{T}_6 \approx$ CCSDTQ5(6) − CCSDTQ5, where in all cases, this contribution is negligible.

TABLE 3: W2.2[e] Total Atomization Energies in kcal/mol

	TAE_e[a]	TAE_0[b]	experiment[c]
SiF_4[f]	578.23	566.36	565.1 ± 1.9, 566.04[41]
PF_5	561.28	545.17	546.0 ± 0.5
SF_6	485.12	465.63	464.9 ± 0.5
$HClO_3$	273.01	257.40	N/A
$HClO_4$	335.35	313.36	N/A[d]

[a] W2.2 Zero-point exclusive, nonrelativistic, clamped-nuclei TAEs for testing/parametrization of DFT functionals. [b] W2.2 relativistic, first-order spin orbit coupling, DBOC TAEs at 0 K. See Supporting Information for details about and source references for the zero-point vibrational energies. [c] From ref 76. [d] Earlier calculation: 313.75 kcal/mol.[57] [e] The SCF component is extrapolated from the aug-cc-pV{5,6}+2d1f basis set pair and not from aug-cc-pV{Q,5}+d as is done in regular W2.2 theory. The latter values underestimate the former by 0.28, 0.31, 0.42, 0.39, and 0.66 kcal/mol for SiF_4, PF_5, PF_6, $HClO_3$, and $HClO_4$, respectively. [f] The corresponding W4lite values are (again with improved SCF component, although here, the difference between the two SCF components is negligible) TAE_e = 578.26 kcal/mol and TAE_0 = 566.40 kcal/mol.

correlated ab initio methods.) We have previously shown[1] that aug-pc3+d is adequate for mapping thermochemistry (%MP2,%HF) surfaces, whereas aug-pc2+2d suffices for barrier heights.

The straits run approximately on a line through the (27,56) and (45,73) points. The global minimum lies at (31,60), previously defined as B2T-PLYP,[1] but the rmsd only rises very slowly from that point along the straits, whereas it rises very steeply in the perpendicular direction.

B. Analysis of Subsets. Figures 2–6 present rmsd surfaces, for B2x-PLYP double hybrids and the aug-pc2 basis sets, for Truhlar's DBH24 (24 diverse barrier heights) benchmark set and the following subsets thereof: HAT, Hxfer, SN2, and UAR. The surface for the W3 set of total atomization energies, obtained by using the aug-pc3 basis set, is depicted in Figure 1. Error statistics for various critical points are summarized in Table 4.

In contrast, the DBH24 and subset surfaces all exhibit basins rather than straits. The UAR basin is the most symmetric, whereas especially the SN2 basin is quite elongated.

Of course, specific extreme points on these surfaces correspond to established methods: (0,50) is equivalent to BH&HLYP (Becke half-and-half LYP), whereas (100,100) is just plain MP2. MP2 yields excellent performance for the SN2 subset but unacceptable results for all the others; it is therefore not particularly surprising that the SN2 optimum lies at very high percentages of MP2-type correlation and HF-type ex-

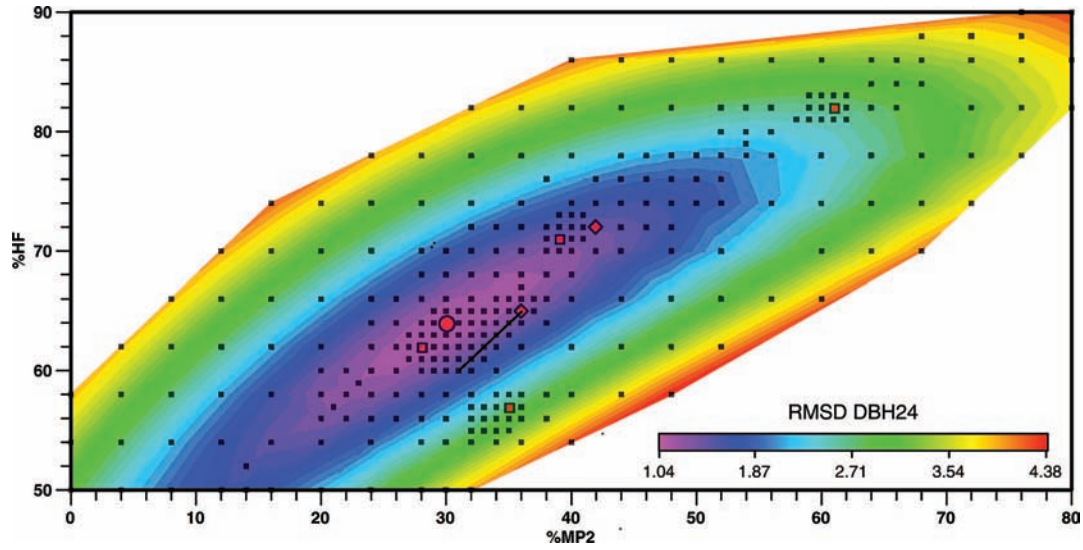

Figure 2. rmsd (kcal/mol) for the DBH24 mixed barrier height data set of double-hybrid B2-PLYP forms as a function of the percentages of MP2-type correlation (abscissa) and HF-type exchange (ordinate). The aug-pc2 basis set was used throughout. In this graph and the subsequent ones, the large round red marker indicates the DBH24 optimum, the smaller red square markers indicate the minima for the individual subsets, and the diamond-shaped markers indicate B2GP-PLYP (36,65) and B2K-PLYP (42,72). The black straight line indicates the optimum straits for equilibrium thermochemistry.

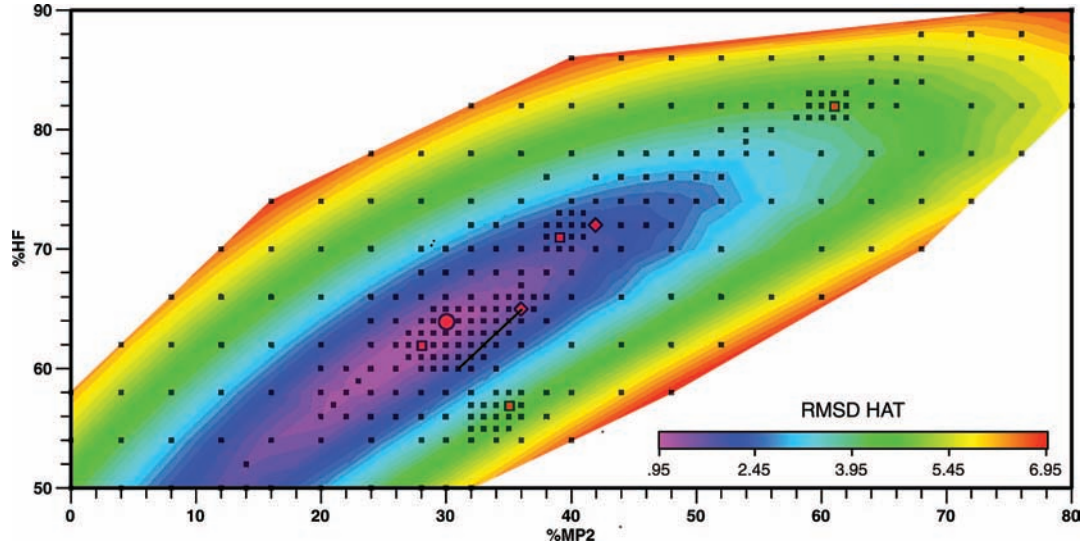

Figure 3. rmsd (kcal/mol) for the HAT barrier heights subset of DBH24 of double-hybrid B2-PLYP forms as a function of the percentages of MP2-type correlation (abscissa) and HF-type exchange (ordinate). The aug-pc2 basis set was used throughout.

change, namely, (61,82). At this point, we have an almost surrealistically low rmsd = 0.15 kcal/mol for the SN2 barriers and a very good performance for Hxfer barriers, but HAT and UAR are actually inferior to BH&HLYP. If one is willing to accept an rmsd for SN2 reactions of up to 1 kcal/mol, a very broad swath of the surface becomes available (Figure 4) which contains the Hxfer and HAT optima as well as a fairly long stretch of the W3 strait but not the UAR optimum.

The optimum for Hxfers lies at (39,71). At this point, excellent rmsds of 0.5 kcal/mol are found for both Hxfer and SN2, whereas the rmsds for HAT and UAR still remain below 2 kcal/mol. This point is a few percent uphill on the W3 canyon; a compromise between thermochemical and Hxfer barrier height performance leads to the B2K-PLYP functional at (42,72), as reported in the previous communication.

The UAR optimum, at (35,57), is too far from both the thermochemistry canyon and the minima for the other reaction classes to be useful in general-purpose thermochemistry and thermochemical kinetics. rmsd for both Hxfer and SN2 exceed 2 kcal/mol, whereas that for HAT reaches 4 kcal/mol. Fortunately, the UAR well is fairly shallow, and optima for Hxfer and especially HAT lie well within its 2 kcal/mol comfort zone.

As expected, the HAT well is by far the steepest. Its optimum, at (28,62), dips below 1 kcal/mol, at the bottom of a rather elongated well. It is well within the comfort zone of all three other classes of reactions, with rmsds of 1.05 kcal/mol for Hxfers, 0.90 kcal/mol for SN2 reactions, and 1.30 kcal/mol for UAR reactions.

Not surprisingly then, the rmsd surface for the DBH24 set overall is dominated by the HAT component, and its minimum at (30,64) is only a slight improvement (0.02 kcal/mol) over the HAT subset minimum. Both the HAT and DBH24 minima are considerably up the W3 canyon walls; thermochemical performance is clearly unacceptable.

The optimum over a sum-square function equally weighted between DBH24 and W3 lies at (36,65). At this point, thermochemical performance over the W3 set is not greatly different from the B2T-PLYP optimum, whereas the DBH24

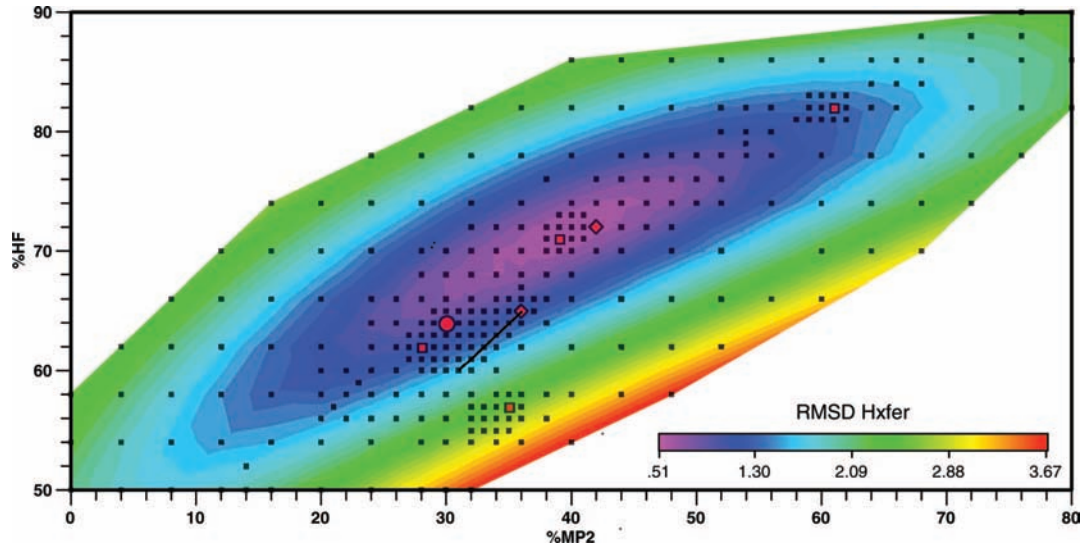

Figure 4. rmsd (kcal/mol) for the Hxfer barrier heights subset of DBH24 of double-hybrid B2-PLYP forms as a function of the percentages of MP2-type correlation (abscissa) and HF-type exchange (ordinate). The aug-pc2 basis set was used throughout.

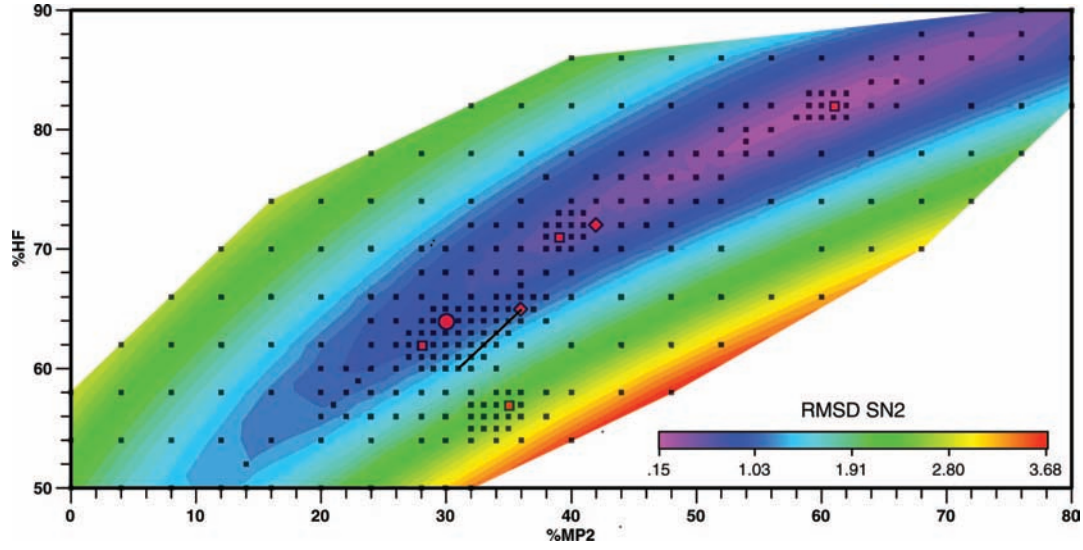

Figure 5. rmsd (kcal/mol) for the SN2 barrier heights subset of DBH24 of double-hybrid B2-PLYP forms as a function of the percentages of MP2-type correlation (abscissa) and HF-type exchange (ordinate). The aug-pc2 basis set was used throughout.

rmsd rises modestly from 1.04 to 1.21 kcal/mol. The only subset of reactions in which this minimum represents a significant deterioration is HAT, for which rmsd goes up from 1.02 to 1.48 kcal/mol—still well below the "magic" 2 kcal/mol and still considerably better than B2T-PLYP, B2K-PLYP, and especially B2-PLYP. We therefore propose the (36,65) point as a general-purpose solution, B2GP-PLYP.

C. Different Semilocal Exchange and Correlation Functionals. Grimme[5] notes in passing that "We tested B88, OPTX, and PBE for exchange and LYP and PBE for correlation in various combinations. All in all, the combination of B88 and LYP yields the best results, although replacing B88 by OPTX gave very similar results. [I]nferior results [were] obtained in preliminary computations with PBE and TPSS."

We considered several combinations for our own reference data sets and can confirm his observations. In addition, we considered several additional correlation functionals (notably PW91c and B95c) and found performance for PW91c-including double hybrids to be clearly inferior as well and this to be even more the case for B95c-including double hybrids. In these various attempts, results were relatively insensitive to the choice of exchange functional.

A referee of ref 1 expressed surprise that B2x-PLYP would turn out to be a felicitous choice because the LYP correlation functional does not satisfy the uniform electron gas limit. In addition, both Grimme and the present authors found O2x-PLYP to work quite well too, yet Handy's O exchange functional does not satisfy the uniform electron gas limit either.

We do note that LYP is rooted in the Colle—Salvetti formula,[79] itself based on correlation from the exact Hartree—Fock orbital in the archetypical two-electron pair correlation system, helium atom. It becomes tempting to speculate that, whatever its shortcomings otherwise, LYP may mesh uniquely well with wave function-based correlation methods.

D. Performance over Various Data Sets. ***1. Total Atomization Energies for the W3 Set.*** The comparisons in Table 5 are made to the nonrelativistic, clamped-nuclei components of the W4 total atomization energies of the molecules in the W4 training set.[38]

We shall focus first on B2x-PLYP. Without CBS extrapolation, B2GP-PLYP narrowly beats B2T-PLYP, followed by B2K-PLYP and finally B2-PLYP. Basis-set sensitivity is similar for B2GP and B2T, pronouncedly stronger for B2K, and weakest

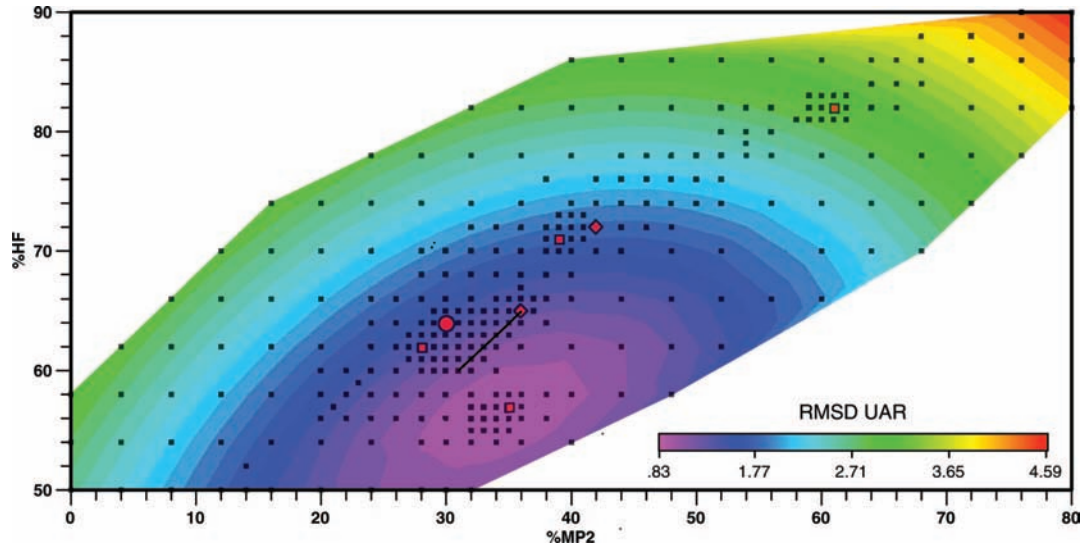

Figure 6. rmsd (kcal/mol) for the UAR reaction barrier heights subset of DBH24 of double-hybrid B2-PLYP forms as a function of the percentages of MP2-type correlation (abscissa) and HF-type exchange (ordinate). The aug-pc2 basis set was used throughout.

TABLE 4: RMSD Deviations (kcal/mol) over the DBH24 Barrier Set, Various Subsets Thereof, and the W3 Set of Total Atomization Energies for Various Critical Points on the B2x-PLYP Surface

(MP2,HF)	description	DBH24	HAT	Hxfer	SN2	UAR	W3 raw	W3 CBS
(30,64)	DBH24 optimum	1.04	1.02	0.88	0.80	1.36	4.80	4.07
(28,62)	HAT6 optimum	1.06	0.95	1.05	0.90	1.30	4.88	4.14
(39,71)	H xfer optimum	1.31	1.86	0.51	0.52	1.69	3.48	2.77
(61,82)	SN2 optimum	2.62	4.15	1.28	0.15	2.95	4.74	6.53
(35,57)	UAR optimum	2.65	3.97	2.50	2.33	0.83	6.40	7.44
(36,65)	B2GP-PLYP	1.21	1.48	1.08	1.02	1.23	2.12	2.30
(42,72)	B2K-PLYP	1.37	1.97	0.54	0.49	1.75	2.44	2.29
(31,60)	B2T-PLYP	1.48	1.86	1.56	1.37	1.03	1.84	2.13
(27,53)	B2-PLYP	2.42	3.43	2.48	2.14	0.96	2.80	3.49
(100,100)	MP2	6.94	11.26	3.83	1.17	7.08	12.27	15.37
(0,50)	BH&HLYP	2.87	4.25	2.01	2.07	2.57	22.31	

for B2-PLYP. It thus marches in lockstep with the percentage of MP2-type correlation, as expected.

Error statistics for B2K improve noticeably if ozone (which has a very strong nondynamical correlation character) is excluded. The deterioration upon including ozone is much less noticeable for the other functionals, suggesting that sensitivity toward nondynamical correlation may be a weaker point of B2K.

With CBS extrapolation, there is little to choose between B2K, B2T, and B2GP at the CBS limit. The weaker basis-set sensitivity of B2T and B2GP may be seen as a plus. B2-PLYP's performance is markedly inferior.

For the mPW2x-PLYP functionals, we can make similar observations, with mPW2-PLYP taking more or less the same place as B2T-PLYP.

2. NHTBH38 and HTBH38 Barrier Height Sets. We will again first consider the B2x-PLYP functionals. B2GP-PLYP obviously puts in the best performance for HAT, edging out B2T-PLYP and being markedly better than B2K-PLYP and especially B2-PLYP. It does second best for SN2 reactions (after B2K-PLYP), outperforming B2T-PLYP and especially B2-PLYP. For UAR reactions, B2GP-PLYP does marginally worse than B2T-PLYP and B2-PLYP but markedly better than B2K-PLYP. The overall ordering of rms deviation for the Truhlar NHTBH38 (non-Hxfer barrier heights) set is B2GP-PLYP < B2T-PLYP < B2K-PLYP < B2-PLYP.

We note in passing a pronounced basis-set sensitivity for the SN2 reactions, seen when comparing aug-pc3 and aug-pc2 results. For the UAR reactions, it is much weaker and even more so for the HATs (somewhat counterintuitively) and Hxfers.

Speaking of the latter, rms deviation for the HTBH38 (Hxfer barrier heights) set is ordered B2K < B2GP < B2T $\ll$ B2. By averaging the NHTBH38 and HTBH38 rms deviations for the aug-pc3 basis set, we obtain the ordering B2GP (1.39) < B2K (1.55) $\lesssim$ B2T (1.63) < B2 (2.49). For the mPW2x-PLYP functionals, the same analysis leads to mPW2GP (1.46) $\lesssim$ mPW2K (1.53) < mPW2-PLYP (2.28).

3. Hydrogen Bonds. When considering the great importance of hydrogen bonding in various fields of chemistry and especially chemical biology, the performance of double hybrids for hydrogen bonds deserves closer scrutiny. An assessment for the 16 hydrogen-bonded complexes of Boese et al.,[70] as well as for the subset of 11 neutral ones, is given in Table 6.

As discussed, for example, by Stone,[106] hydrogen bonds have a nontrivial dispersion component, but the latter is not the main glue holding hydrogen bonds together. As such, one would expect double hybrids to represent an incremental improvement over conventional DFT functional. In fact, we see in Table 6 that all double hybrids not only yield excellent performance (rmsd of 1 kJ/mol or less) for the neutral hydrogen-bonded complexes but actually outperform MP2, which is widely considered to be a benchmark-quality method for hydrogen bonds. Almost all methods deteriorate in performance, to a greater or lesser extent, when the charged complexes are included: nearly all of this deterioration is on account of the protonated water dimer, $(H_2O)_2H^+$, which is very strongly bound. Even so, the 0.76 kcal/mol overestimate in B2GP-PLYP for this system only represents a relative error of 2.2%. In fact,

TABLE 5: RMS Errors of Various Functionals (in kcal/mol)[a]

	B2-PLYP	B2-PLYP	B2-PLYP	**B2GP-PLYP**	PBE2K-PLYP	O2K-PLYP	mPW2GP-PLYP	mPW2-PLYP	mPW2K-PLYP	B3LYP	PBE0	B97−1	BMK	M06L	M06	M06−2X
BH6/apc-2	2.48	0.54	1.44	**1.08**	0.63	0.65	1.26	1.93	0.72	5.24	5.08	5.06	1.97	5.08	1.97	1.43
W3/apc2+d	2.54(2.58)	4.05(3.58)	3.08(2.84)	**3.08(2.82)**	3.00(2.65)	4.67(4.10)	3.05(2.70)	3.11(2.79)	3.49(3.05)	3.59	3.91	3.87	3.58	5.22	3.56	3.98
W3/apc3+d	2.55(2.59)	2.84(2.30)	2.15(1.92)	**2.13(1.86)**	2.34(2.05)	3.42(2.82)	2.18(1.84)	2.29(1.97)	2.44(1.98)	3.19	3.66	4.01	3.47	4.91	3.38	3.83
W3/apc4	2.68(2.72)	2.58(2.05)	2.04(1.83)	**1.86(1.78)**			2.09(1.79)	2.20(1.90)	2.27(1.84)							
W3/apc2+d/CBS10	3.63(3.65)	2.72(2.57)	2.59(2.57)	**2.76(2.75)**	3.58(3.60)	2.82(2.57)	2.89(2.86)	2.60(2.49)	2.99(2.93)							
W3/apc3+d/CBS15	3.12(3.15)	2.36(1.97)	2.12(2.00)	**2.17(2.07)**	2.82(2.74)	2.69(2.20)	2.32(2.18)	2.25(2.05)	2.40(2.16)							
W3/apc4/CBS20	2.98(3.01)	2.33(1.89)	2.04(1.91)	**2.05(1.91)**			2.16(1.97)	2.19(1.96)	2.24(1.94)							
Non-Hxfer Reactions																
HAT	4.16(4.02)	3.10(3.30)	2.71(2.65)	**2.48(2.51)**	3.12	3.29	2.51(2.54)	4.93(3.54)	3.00(3.17)	9.12	7.53	6.48	2.28	8.08	4.42	2.27
SN2	1.92(1.72)	0.50(0.49)	1.18(0.99)	**0.96(0.71)**	0.72	1.42	1.03(0.73)	2.64(1.40)	0.59(0.46)	2.91	1.59	2.73	1.78	2.56	1.42	1.68
UAR	1.12(1.06)	1.67(1.56)	1.09(0.99)	**1.24(1.11)**	1.82	2.03	1.28(1.14)	1.62(1.15)	1.63(1.50)	2.95	2.71	2.13	1.61	2.20	1.91	1.05
NHTBH38//BMK	2.71(2.58)	1.97(2.04)	1.79(1.70)	**1.65(1.59)**	2.03	2.31	1.69(1.62)	2.40(2.27)	1.92(1.96)	5.66	4.57	4.19	1.91	4.97	2.82	1.76
Weak Interactions																
HB6	0.17(0.41)	0.55(0.20)	0.26(0.29)	**0.38(0.23)**	1.07	0.68	0.73(0.35)	0.56(0.32)	0.83(0.38)	0.96	0.36	0.48	0.84	0.26	0.37	0.25
CT7	0.86(0.74)	0.77(0.65)	0.76(0.64)	**0.78(0.66)**	1.08	0.60	1.07(0.95)	1.11(0.96)	1.04(0.92)	0.91	1.33	1.38	0.58	1.79	0.79	0.44
DI6	0.34(0.35)	0.32(0.32)	0.29(0.28)	**0.28(0.27)**	0.60	0.36	0.43(0.43)	0.33(0.30)	0.49(0.50)	0.85	0.44	0.39	0.83	0.51	0.38	0.32
WI9	0.26(0.44)	0.22(0.22)	0.19(0.36)	**0.18(0.30)**	0.35	0.21	0.33(0.15)	0.30(0.21)	0.37(0.12)	0.80	0.45	0.38	0.98	0.29	0.29	0.26
Nonbonded int.//BMK	0.50(0.52)	0.50(0.40)	0.43(0.43)	**0.46(0.41)**	0.81	0.48	0.69(0.55)	0.66(0.54)	0.71(0.56)	0.87	0.76	0.78	0.83	0.95	0.53	0.34
Hxfer																
HTBH38/apc2	2.43(2.39)	0.86(0.82)	1.59(1.55)	**1.19(1.15)**	0.92	0.99	1.34(1.29)	2.33(2.29)	0.96(0.91)	5.15	4.98	5.22	1.88	5.11	2.57	1.57
Pd-reactions	0.98	1.17	0.85	**0.84**	2.13	2.05	0.90	0.88	1.08	2.22	0.79	1.92	7.25	1.54	5.84	8.42
(w/o complexes)	0.91	1.18	0.57	**0.71**	2.35	2.16	0.93	0.73	1.18	1.78	0.66	1.89	8.34	1.34	6.66	8.87

[a] Double-hybrid definitions: B2-PLYP, (53,27); B2T-PLYP, (60,31); B2K-PLYP, (72,42); **B2GP-PLYP, (36,65)**; mPW2-PLYP, (55,25); mPW2K-PLYP, (72,42). Values in parentheses for the W3 set are exclusive of ozone. For this molecule, post-CCSD(T) correlation effects account for over 3 kcal/mol of the total atomization energy.[38] Values in parentheses for the HTBH38, NHTBH38, and nonbonded interactions sets are with the aug-pc3+d basis set, others are with the aug-pc2 + 2d basis set. For approximate mean absolute deviations, multiply by 0.6745 (Huber, P. J. *Robust statistics*; Wiley-IEEE, 2004; p 108.

TABLE 6: Performance Statistics (kcal/mol) of Various Functionals for the Set of 16 Hydrogen Bonds of Boese et al.[70] and for the Subset of 11 Neutral Species[a]

	11 neutral complexes			all 16 complexes		
	rmsd	MSD	MAD	rmsd	MSD	MAD
B2GP-PLYP/apc3+d raw	0.18	0.07	0.15	0.30	0.16	0.22
B2T-PLYP/apc3+d raw	0.18	0.02	0.15	0.26	0.07	0.20
B2T-PLYP/apc3+d-CBS15val	0.20	0.05	0.17	0.29	0.11	0.22
B2-PLYP/apc3+d-CBS15val	0.20	−0.02	0.17	0.28	0.01	0.20
B2GP-PLYP/apc3+d-CBS15val	0.21	0.10	0.17	0.26	0.11	0.20
B2K-PLYP/apc3+d raw	0.21	0.12	0.17	0.27	0.17	0.21
M06/apc2+2d	0.21	−0.15	0.17	0.44	−0.04	0.29
B2K-PLYP/apc3+d-CBS15val	0.24	0.16	0.20	0.33	0.22	0.25
B2-PLYP/apc3+d raw	0.28	0.01	0.20	0.30	0.04	0.22
MP2/apc3+d	0.29	0.15	0.21	0.31	0.16	0.25
M06−2X/apc2+2d	0.31	0.19	0.23	0.92	0.53	0.56
B3LYP/apc2+2d	0.35	−0.16	0.26	0.45	−0.02	0.28
M06L/apc2+2d	0.37	0.06	0.28	0.50	0.01	0.38
X3LYP/apc2+2d	0.39	0.20	0.31	0.61	0.37	0.44
B97−1/apc2+2d	0.42	0.29	0.31	0.61	0.44	0.45
SCS-MP2/apc3+d	0.46	−0.40	0.41	0.68	−0.55	0.56
BMK/apc2+2d	0.50	−0.36	0.42	0.52	−0.40	0.44
PBE0/apc2+2d	0.58	0.35	0.41	0.97	0.66	0.70
M06HF/apc2+2d	0.64	−0.06	0.48	1.86	0.72	1.10
B3PW91/apc2+2d	0.71	−0.58	0.65	0.70	−0.32	0.60
B97-2/apc2+2d	0.72	−0.67	0.67	0.68	−0.56	0.64

[a] The entries have been sorted by increasing rmsd for the 11 neutral species.

the rms percentage error for B2GP-PLYP goes down from 3.9% to 3.3% upon inclusion of the ionic species.

As an additional test, we considered an even more strongly bound ionic complex, namely FHF^-. Bonding in this complex was recently reviewed by Davidson;[107] our W2.2 calculation yields D_e = 44.16 kcal/mol valence only, 44.21 kcal/mol including inner-shell correlation, and 44.18 kcal/mol additionally including relativistic effects. The B2GP-PLYP value, by way of illustration, is 44.31 kcal/mol raw and 44.37 kcal/mol with CBS extrapolation. Within the harmonic oscillator approximation, the CCSD(T)/A′VQZ zero-point vibrational energy difference is −0.52 kcal/mol, leading to a W2.2 D_0 = 43.65 kcal/mol, in good agreement with the experimental D_0 = 44.4 ± 1.6 kcal/mol.[108]

4. van der Waals Complexes. We will now turn to Zhao and Truhlar's weak interactions benchmark set.[80] Some caution is due here, because the energetics of van der Waals complexes are generally driven by dispersion above other factors. Dispersion in the large R limit is at least arguably[83,84] beyond the capabilities of DFT as the term is generally understood. At medium range, where repulsion and overlap are significant, things are not as clear-cut (see, e.g., refs 15–18 and 82).

A pragmatic approach has been[84–87] the use of empirical corrections based on Lennard-Jones-type potentials multiplied by a cutoff function (e.g., a Fermi function) that goes to unity at the long internuclear distance limit and to zero at the short distance limit. These were shown[84–88] to considerably improve performance of DFT[84–87] and double-hybrid[88] functionals for van der Waals complexes. Of course, double hybrids should already partially recover dispersion, which is reflected in the fact that a +D correction for B2-PLYP requires an empirical damping factor, s_6 = 0.55, compared to s_6 = 1.05 for B3LYP.[88] The specific form and atomic parameters that we use are those in Grimme.[87]

In the present work, we have optimized s_6 values for our double hybrids, as well as for the conventional DFT functionals B3PW91, PBE0, BMK, X3LYP,[92] M06L, M06, and M06−2X, by using a procedure intended to be as compatible as possible with the earlier determinations of Grimme[88] for B2-PLYP and mPW2-PLYP (see also ref 87 for B3LYP). Preliminary optimization for the WI9 subset of Zhao and Truhlar revealed that dispersion corrections are too small to yield stable s_6 coefficients over such a small sample. Instead, as in ref 88, we employed the S22 benchmark set by Hobza and co-workers,[81] which includes systems as large as (adenine)(thymine) and $(uracil)_2$ (both hydrogen-bonded and stacked dimers), for which unscaled Grimme corrections are as large as 10 kcal/mol. The same TZVPP[89] basis set as that in ref 88 was employed; because it is well-known (e.g., ref 91) that basis-set convergence for weak interaction energies tends to be from above for raw energies and from below with Boys−Bernardi[90] counterpoise correction, we considered the average of uncorrected and corrected energies, then minimized rmsd with respect to s_6. The final s_6 was then rounded up to the nearest multiple of 0.05. We verified that, in this manner, we were able to to reproduce Grimme's[87,88] s_6 values of 1.05 for B3LYP, 0.55 for B2-PLYP, and 0.40 for mPW2-PLYP. Optimized s_6 values for the other functionals, as well as error statistics over the S22 set with and without correction, can be found in Table 7.

With some reservations, small s_6 values can be seen as an indication of a functional's ability to cope with dispersion. By this token, PBE0 and especially BMK (note the small rmsd of only 0.6 kcal/mol after correction) appear to be superior to B3LYP. Note the conspicuously low s_6 values for the M06 family (0.20 for M06L, 0.25 for M06); in the case of M06-2X, the small s_6 value and marginal improvement in rmsd upon its inclusion suggest that a dispersion correction for M06-2X amounts to gilding the lily, and we recommend omitting it for this functional. While Grimme's correction still appears to be beneficial for the other functionals, the claim that the M06 family can handle weak interactions is at least empirically justified by the present results.

Naively, one might expect MP2 to perform excellently for dispersion-driven complexation energies. In fact, however, this is not the case for the aromatic systems in S22 and particularly not for the stacked nucleic acid dimers. Hobza and co-workers[81] found CCSD(T)−MP2 differences as large as 3 kcal/mol, with MP2 systematically overestimating the differences. In fact, as seen in Table 7, one could improve the rmsd over the S22 set at the MP2 basis-set limit by subtracting Grimme's correction (s_6 = −0.22, a similarly anomalous s_6 = −0.16 being obtained for the TZVPP basis set). What such an unphysical correction would really do, of course, is mitigate the overbinding in the aromatic (and especially π-stacked) complexes at the expense of the others. We note that for the S22 set, the uncorrected M06 family of functionals meets (or, in the case of M06-2X, exceeds) the MP2 standard; upon inclusion of a dispersion correction,

TABLE 7: s_6 Parameters and rmsd (kcal/mol) with and without s_6 Correction for the S22 Set of Weakly Interacting Systems of Hobza and Co-workers[a]

		uncorrected			corrected		
functional	s_6	raw	CP	avg	raw	CP	avg
B3LYP	1.05[87]	4.77	5.12	4.95	0.81	0.51	0.66
B3PW91	1.10	5.19	5.50	5.34	0.75	0.53	0.62
X3LYP	0.85	4.15	4.49	4.32	1.03	0.82	0.90
PBE0	0.70	3.37	3.65	3.51	1.10	0.89	0.98
BMK	0.65	2.99	3.34	3.16	0.69	0.55	0.59
M06L	0.20	0.91	1.26	1.08	0.47	0.43	0.40
M06	0.25	1.12	1.58	1.35	0.40	0.44	0.33
M06-2X	(0.06)[b]	0.50	0.63	0.54	0.48	0.43	0.45
B2-PLYP	0.55[88]	1.67	2.36	2.00	0.72	0.39	0.39
B2T-PLYP	0.48	1.90	2.67	2.28	0.78	0.38	0.43
B2GP-PLYP	0.40	1.53	2.35	1.92	0.75	0.42	0.38
B2K-PLYP	0.30	1.09	1.95	1.50	0.72	0.50	0.36
mPW2-PLYP	0.40[88]	1.77	2.42	2.08	0.88	0.63	0.64
mPW2GP-PLYP	0.28	1.11	1.84	1.44	0.83	0.56	0.52
MP2	(−0.16)[c]	1.59	0.90	1.06	(0.89)	(1.15)	(0.71)
MP2@CBS limit[81]	(−0.22)[c]	1.22	1.22	1.22	(0.53)	(0.53)	(0.53)
SCS-MP2	(0.17)[c]	0.76	1.94	1.27	(1.01)	(1.34)	(0.92)

[a] s_6 parameters without a bibliographic reference were obtained in the present work. The TZVPP basis set as employed in ref 88 was used throughout. raw and CP indicate calculations without and with Boys−Bernardi counterpoise corrections, respectively. avg indicates averages of raw and corrected values (which generally converge to the basis set limit from opposite directions[91]). [b] In light of the negligible improvement resulting from including Grimme's correction for M06-2X, we suggest omitting it for this functional. [c] Not intended or recommended as actual corrections, but merely as probes for average under- or overcorrection for dispersion.

both the M06 family and our double hybrids handily outperform MP2 and even SCS-MP2.

As expected, s_6 for the B2x-PLYP family becomes progressively smaller with higher percentage of MP2-like correlation. In fact, the five s_6 values available (including 1.05 for B3LYP, i.e, 0% MP2 correlation), exhibit a nearly perfect linear relationship with this percentage ($s_6 \approx 1.05 - 0.018 \times$ %MP2, $R^2 = 0.9992$). If fitted against the WI9 set of Truhlar instead (here, we used aug-pc3+d basis sets, in order to essentially make counterpoise corrections unnecessary), the relationship is $s_6 \approx 0.91 - 0.0163 \times$ %MP2, with $R^2 = 0.999$.

Interestingly, mPW2-PLYP and mPW2GP-PLYP, after correction, both exhibit weaker performance than the B2-PLYP and M06 families. All of these have dispersion-corrected rmsd values in the range 0.3−0.45 kcal/mol. More detailed comparisons would certainly require a basis set closer to the one-particle limit, which we have not explored because of computational resources.

5. Prototype Reactions at Pd. As stated in the Introduction, one of our aims in developing these double hybrids was to have a functional that would treat barrier heights at transition metals as well as main-group barrier heights. For this purpose, we consider a number of prototype C−C, C−H, and C−X forward and reverse activation barriers at Pd(0), for which we previously[34] obtained basis set limit ab initio data. Our findings are summarized in Table 5.

In our preliminary communication, we found B2K-PLYP to have an rmsd of about 1.2 kcal/mol, somewhat worse than that of the best performer (PBE0, at 0.7 kcal/mol) but still considerably better than those of B3LYP and B97-1 (about 2 kcal/mol) and especially better than those of the kinetics-friendly meta-GGAs BMK (7 kcal/mol), M06 (6 kcal/mol), and M06−2X (8 kcal/mol), all of which fail dramatically. In the present work, we find that B2GP-PLYP yields results basically on par with PBE0 while obviously drastically outperforming the latter on thermochemistry and main-group thermochemical kinetics. mPW2GP-PLYP (rmsd = 0.9 kcal/mol) also performs quite creditably.

Among the various double hybrids, we find the orderings B2GP ≈ B2T < B2 < B2K and mPW2 ≈ mPW2GP < mPW2K. When considering the data at hand together with the HTBH38 and NHTBH38 sets, B2GP emerges as a clear winner, followed by B2K.

6. Performance for the BMK Data Set. Performance for the BMK data set of 474 systems[14] and various subsets thereof is summarized in Tables S-1 and S-2 of the Supporting Information. In these tables, there is little to choose between B2GP-PLYP and B2K-PLYP. B2-PLYP actually edges out both on the overall error, essentially because of its superior performance for anions (where the higher percentages of HF exchange in B2GP-PLYP and B2K-PLYP are a liability, see ref 34).

However, like for barrier heights, it can be argued that comparisons between computed (nonrelativistic) and experimental (relativistic) atomization energies are basically an exercise in comparing apples with oranges.[93] This is especially true because the assumption that the relativistic contributions are much smaller than the residual error in the calculation clearly no longer holds for the double-hybrid functionals.

7. Performance for the W4-08 Neutral Molecule Set. In order to make a more meaningful comparison— to improve the signal-to-noise ratio, as it were—we have assembled a new data set of 100 neutral molecules for which we have W4 total atomization energies available and are using the same nonrelativistic, clamped-nuclei components as our thermochemical reference data. Details of this W4-08 set and references for the individual values can be found in the Supporting Information.

Performance for various double hybrids with different basis sets and with and without explicit inner-shell correlation is summarized in Table 8, together with data obtained by a variety of ab-initio-based computational thermochemistry methods. We are considering two subsets of the W4-08 set:

(a) non-MR (nonmultireference), where all systems with a %[(T)] diagnostic[38] in excess of 10 have been excluded, namely, B_2, Be_2, BN($a^1\Sigma^+$), BN($X^3\Pi$), C_2($X^1\Sigma_g^+$), Cl_2O, ClOO, OClO, F_2, OF, F_2 O, FO_2, FOOF, O_3, S_3, and S_4

TABLE 8: Performance Statistics (kcal/mol) of Various Methods for the W4-08 Set[a]

	polar			non-MR			all		
	rmsd	MSD	MAD	rmsd	MSD	MAD	rmsd	MSD	MAD
BP86	11.16	6.81	8.69	14.78	11.77	12.20	18.05	12.50	14.21
BB95	14.45	10.89	11.01	14.74	10.33	11.40	19.04	11.91	14.16
PBE	13.21	8.48	9.89	14.18	9.37	11.16	18.07	10.80	13.64
mPW1K	16.95	−14.34	14.34	12.98	−10.80	10.86	16.07	−12.81	12.89
KMLYP	7.66	0.87	5.77	10.75	3.61	7.81	13.31	0.09	9.52
TPSS25TPSS	15.29	−12.76	12.76	10.75	−6.09	8.59	12.37	−7.62	9.77
TPSS	15.29	−12.76	12.76	10.75	−6.09	8.59	12.37	−7.62	9.77
PWB6K	10.35	−7.98	8.17	8.50	−6.63	6.88	11.86	−8.63	8.83
BLYP	6.98	−1.53	4.54	8.09	2.67	5.70	12.05	3.51	7.44
B97-K	11.52	−9.21	9.42	7.67	−2.71	5.78	10.14	−4.33	7.04
BB1K	9.64	−7.78	7.79	7.54	−5.90	6.15	10.35	−7.56	7.77
TPSS33B95	9.00	−6.88	7.03	7.36	−5.00	5.97	9.23	−6.22	7.05
TPSS25KCIS	11.37	−9.48	9.48	6.75	−3.96	5.00	8.24	−5.03	6.03
HCTH407	6.08	0.42	4.61	5.98	−0.91	4.42	7.73	0.43	5.48
TPSSh	8.54	−7.02	7.02	5.88	−0.99	4.45	6.36	−1.23	4.62
M06L	6.24	−0.34	4.99	5.72	0.20	4.36	5.94	0.61	4.57
TPSS21KCIS	9.66	−8.00	8.02	5.52	−2.63	3.95	6.54	−3.34	4.61
mPW1PW91	8.15	−6.65	6.70	5.39	−3.93	4.15	6.48	−4.39	4.71
TPSS25B95	5.66	−3.98	4.25	4.85	−2.38	3.72	5.93	−2.92	4.10
B3LYP	7.99	−6.14	6.23	4.82	−1.24	3.43	5.82	−1.80	3.93
X3LYP	7.64	−5.79	5.90	4.65	−1.27	3.30	5.78	−1.92	3.83
mPW25B95	4.18	1.58	3.28	4.53	2.31	3.31	5.22	2.23	3.79
M05-2X	5.38	0.39	4.19	4.47	−1.67	3.36	6.98	−3.13	4.54
PBE0	6.22	−4.05	4.89	4.37	−1.67	3.31	5.24	−2.00	3.60
TPSS1KCIS	6.42	−4.95	5.20	4.26	0.10	3.16	4.81	0.06	3.40
B33B95	5.70	−4.29	4.32	4.12	−2.71	3.24	5.80	−3.52	3.97
TPSS20B95	3.85	−2.10	3.04	4.04	−0.69	2.97	4.85	−0.83	3.31
B3PW91	6.23	−4.59	4.78	3.92	−1.30	2.87	4.80	−1.49	3.22
M05	3.52	−0.19	2.62	3.90	−0.76	2.67	4.88	−1.58	3.28
M06	4.19	1.37	3.36	3.87	0.58	2.68	4.60	−0.13	3.13
B97-1	3.64	−1.39	2.90	3.73	−0.55	2.90	4.68	−0.44	3.30
B97-2	3.90	−1.90	3.26	3.72	−0.58	2.86	4.46	−0.71	3.12
tHCTHh	3.32	0.34	2.96	3.57	−0.48	2.92	4.84	−0.09	3.54
mPW28B95	3.50	0.25	2.78	3.54	1.12	2.49	4.44	0.78	2.89
B97-3	5.37	−3.76	4.25	3.39	−0.86	2.56	4.62	−1.38	2.99
B1B95	4.04	−2.28	3.06	3.25	−0.89	2.42	4.35	−1.27	2.70
VSXC	3.09	0.45	2.56	3.18	0.14	2.46	3.96	0.40	2.90
M06-2X	3.86	−0.86	2.77	3.11	−0.96	2.06	7.04	−2.51	3.54
B98	4.14	−2.61	2.98	3.08	−1.30	2.27	4.49	−1.57	2.80
mPW1B95	3.57	−1.06	2.85	3.06	−0.06	2.17	4.40	−0.66	2.58
BMK	3.95	0.62	3.29	3.01	−0.08	2.43	5.73	−1.38	3.50
B2 apc3 CBS15	2.60	0.30	2.04	2.94	1.47	2.17	3.03	1.17	2.20
mPW2K apc3 CBS15	3.73	2.36	2.84	2.81	1.14	2.12	3.69	0.19	2.66
PW6B95	3.85	−2.27	2.67	2.68	−0.35	1.91	4.06	−0.93	2.35
G2	3.73	−1.88	2.68	2.60	−1.45	1.84			
B2 apc3 raw	2.66	−0.58	2.07	2.45	0.65	1.79	2.66	0.33	1.89
B2K apc3 raw	2.48	−0.25	2.01	2.39	−1.09	1.87	4.07	−2.08	2.75
B2K apc3 CBS15	3.08	1.37	2.51	2.39	0.31	1.81	3.68	−0.67	2.49
mPW2 apc3 CBS15	2.66	−0.84	2.16	2.33	0.46	1.88	3.15	−0.27	2.33
G3B3	3.35	−2.59	2.64	2.23	−1.39	1.57	2.47	−1.53	1.74
B2GP apc3 CBS15	2.34	0.45	1.97	2.19	0.63	1.75	2.96	−0.10	2.19
G2MP2	2.71	−0.41	2.06	2.13	−0.80	1.71			
B2T apc3 CBS15	2.37	−0.32	2.06	2.09	0.36	1.70	2.87	−0.32	2.12
mPW2GP apc3 CBS15	2.39	−0.12	2.09	2.07	0.09	1.66	3.26	−0.75	2.28
B2T apc3 raw	2.81	−1.36	2.34	2.05	−0.61	1.60	3.10	−1.30	2.19
B2GP apc4 CBS20				2.01	0.33	1.54			
B2GP apc3 raw	2.35	−0.46	2.04	1.94	−0.45	1.54	3.11	−1.20	2.16
B2GP apc4 raw				1.85	−0.13	1.42			
G3	2.32	−1.09	1.37	1.79	−0.96	1.28			
G4	1.96	−1.33	1.46	1.25	−0.50	0.90	1.31	−0.52	0.95
G3X	1.65	−0.84	1.21	1.22	−0.34	0.91	1.27	−0.40	0.96
CBS-QB3	1.58	−0.43	1.10	1.14	−0.39	0.86	1.36	−0.48	0.96
W1Usc	0.77	0.19	0.65	0.56	−0.03	0.41	1.07	−0.27	0.61
W2.2	0.38	−0.11	0.28	0.40	−0.21	0.28	0.92	−0.45	0.52
W3.2	0.20	−0.06	0.15	0.23	−0.11	0.16	0.42	−0.16	0.22
W4lite	0.17	0.06	0.14	0.21	−0.07	0.14	0.29	−0.10	0.17

[a] The entries have been sorted by descending order of rmsd for the non-MR subset.

(b) polar, including the following systems with highly polar bonds: $AlCl_3$, AlCl, AlF_3, AlF, BeF_2, $BeCl_2$, BF, BF_3, BHF_2, CCl_2, CF_2, CF_4, CO_2, HCl, HF, SiO, SO, SO_2, and SO_3.

Eliminating highly multireference systems has a pronounced effect on error statistics, especially for B2K-PLYP, less so for B2GP-PLYP, and least for B2-PLYP.

In the table and the following discussion, the notation CBS*n* denotes a Petersson complete basis set pair extrapolation[94] with the minimum number of pairs parameter N_{min} set to *n*. Professor Petersson recommends setting the pair extrapolation parameter N_{min} to 5 for an spd basis set, 10 for an spdf basis set, 15 for an spdfg basis set, and 20 for an spdfgh basis set.[95] We have followed this recommendation in the present work.

aug-pc3+CBS15 appears to be adequate to reach the one-particle basis-set limit, although aug-pc2+CBS10 will apparently do in a pinch.

Near the CBS limit, polar systems are not greatly worse than the norm for B2GP-PLYP, whereas marked deterioration is seen in B2K-PLYP. This is additional evidence that although B2K-PLYP may perform comparably to B2GP-PLYP in favorable cases, B2GP-PLYP is the more robust of the two functionals.

By considering signed errors at the CBS limit, we note a marked overshoot in B2-PLYP, whereas raw and CBS20 extrapolated B2GP-PLYP/aug-pc4 data on average closely bracket the true total atomization energies. mPW2K-PLYP overbinds at the basis-set limit, and we can no longer recommend it. mPW2GP-PLYP performs comparably to B2-PLYP.

How does B2GP-PLYP stack up compared to wave function ab-initio-based computational thermochemistry protocols? As can be seen in Table 8, it actually outperforms G2 theory and stacks up in the neighborhood of G3 theory and G3B3 theory (around 2 kcal/mol rmsd on the non-MR subset). G3X, G4, and CBS-QB3 are all superior, with rmsds on the same set hovering around the 1.2 kcal/mol mark. W1Usc, the variant of W1 theory implemented into Gaussian 03, yields rmsd = 0.56 kcal/mol and MAD = 0.41 kcal/mol, quite close to the 0.37 kcal/mol reported in the original W1 paper[35] for a much smaller sample. A somewhat slight further reduction is achieved by going up to W2.2 theory (mostly on account of molecules like CF_4 with very slow basis-set convergence), whereas cutting rmsds to the kJ/mol level requires inclusion of post-CCSD(T) correlation effects (as done in W3.2, W4lite, and of course full W4) even for these species. Inclusion of molecules with strong nondynamical correlation doubles the rmsds for W1Usc and W2.2 but affects those for W3.2 and W4lite much more modestly; robustness against such effects clearly requires post-CCSD(T) corrections. For G3X, G4, and CBS-QB3, the post-CCSD(T) errors are on a scale similar to that of the remaining errors in the method, and deterioration is thus fairly inconspicuous.

E. Highly Polar and/or Pseudohypervalent Compounds. A referee of our preliminary communication raised the issue that popular DFT functionals like B3LYP tend to perform very poorly for hypervalent molecules such as SF_6 and PF_5. This issue went unaddressed in the communication because of lack of space; we shall consider it here.

First, a point of terminology seems in order. It was conclusively shown (see, e.g., the work of Cioslowski and Mixon;[96] additional references can be found in ref 57) that many such molecules are not hypervalent in the narrow sense of the word; that is, no d-hybridization needs to be invoked to explain their bonding pattern. What molecules such as AlF_3, SiF_4, PF_5, SF_6, SO_2, SO_3, and $HClO_4$ (and, to a much lesser extent, AlF, SiO, SO) have in common is a situation where a central second-row atom in a high oxidation state has 3d Rydberg orbitals that are low-lying enough to accept strong back donation from chalcogen and halogen lone pair orbitals. We prefer the terms "pseudohypervalent" or "d-backbonding" compounds.

Second, some care must be taken here not to conflate several superficially related issues. First of all, there is the question whether the problem is specific to pseudohypervalent compounds or whether it more generally occurs for polarly bound molecules (such as, e.g., BF_3 and CF_4). But second, if pseudohypervalence is indeed involved, it has been well established[57,72,97,98] that typical Gaussian basis sets are sorely lacking in high-exponent d functions—for Cl_2O_7, the most extreme example thus far documented, adding a series of tight d functions to the aug-cc-pVDZ basis set increases the total atomization energy by over 100 kcal/mol![57] (Essentially all of this effect is recovered at the SCF level.)

In short, one has to be careful to distinguish between basis-set incompleteness, inability to cope with highly polar bonds, and inability to cope with pseudohypervalence. All basis sets used in the present work were adequately supplemented with high-exponent d functions on the second-row elements, such that this issue can be regarded as eliminated. This leaves the two remaining ones.

Considering, for example, the B3LYP functional, we do find dismayingly large errors in the computed total atomization energy for systems such as $HClO_4$ (−22 kcal/mol), SF_6 (−21 kcal/mol), PF_5 (−17 kcal/mol), SiF_4 (−20 kcal/mol), SO_3 (−16 kcal/mol), SO_2 (−10 kcal/mol), or AlF_3 (−13 kcal/mol). Yet, we also find significant errors in systems such as BF_3 (−6 kcal/mol) and CF_4 (−10 kcal/mol) which cannot plausibly be described as hypervalent or pseudohypervalent. Some, but not all, of these errors drop significantly when the PW91 correlation functional is substituted for LYP, and all of them drop significantly with the B95 correlation functional. Yet, even B1B95 retains errors of −11 kcal/mol for AlF_3, −14 kcal/mol for SiF_4, and −8 kcal/mol for $HClO_4$, although it has no trouble coping with BF_3 (−2 kcal/mol) and CF_4 (+1 kcal/mol) and in fact overestimates binding on PF_5 (+6 kcal/mol).

The double hybrids go a long way in remedying these particular weaknesses of the underlying functional. At the B2GP-PLYP/aug-pc3+d+CBS15 level, BF_3 (+2.4 kcal/mol) and CF_4 (−1.7 kcal/mol) do not seem to present any specific problem, but neither do AlF_3 (−0.2 kcal/mol), SiF_4 (+2.8 kcal/mol), PF_5 (+2.2 kcal/mol), SF_6 (+1.8 kcal/mol), SO_2 (−0.7 kcal/mol), SO_3 (−1.6 kcal/mol), $HClO_2$ (+0.2 kcal/mol), or $HClO_3$ (+0.2 kcal/mol). Only $HClO_4$ (−4.3 kcal/mol) is clearly a bit much to handle.

B2K-PLYP clearly is more vulnerable, with errors of +6.3 kcal/mol for CF_4, +5.1 kcal/mol for SiF_4, +4.2 kcal/mol for PF_5, and +3.8 kcal/mol for SF_6. As we noted above that the energetic consequences of pseudohypervalence almost exclusively manifest themselves at the SCF/DFT level, their recuperation should not be affected to this degree by what is, in the larger scheme of things, a fairly subtle shift in the correlation treatment. However, it is well-known that MP2 tends to severely overestimate the correlation energy of systems with highly polar bonds, and thus, it would stand to reason that a method with a comparatively large percentage of MP2-like correlation would inherit this deficiency.

TABLE 9: Basis-Set Convergence and Effect of Explicit Inner-Shell Correlation for the B2GP-PLYP Functional[a]

	all-electron			valence only		
	rmsd	MSD	MAD	rmsd	MSD	MAD
apc2+2d raw	3.12	−1.90	2.44	3.12	−1.47	2.33
apc2+2d CBS10	2.86	0.97	2.24	2.32	−0.84	1.81
apc3 raw	1.94	−0.45	1.54	2.44	−1.58	1.93
apc3 CBS15	2.19	0.63	1.75	1.92	−0.50	1.54
apc4 raw	1.85	−0.13	1.42			
apc4 CBS20	2.01	0.33	1.54			
aug-cc-pV(T+d)Z raw				4.70	−4.05	4.08
aug-cc-pV(T+d)Z CBS10				2.71	−1.86	2.16
aug-cc-pV(Q+d)Z raw				2.54	−1.71	2.04
aug-cc-pV(Q+d)Z CBS15				1.98	−0.63	1.58
aug-cc-pwCVTZ raw	3.99	−3.36	3.43	4.25	−3.67	3.71
aug-cc-pwCVTZ CBS10	2.35	−1.20	1.79	2.42	−1.59	1.94
aug-cc-pwCVQZ raw	2.28	−1.28	1.80	2.41	−1.60	1.94
aug-cc-pwCVQZ CBS15	1.99	−0.19	1.61	1.91	−0.58	1.53
MG3S raw	5.15	−3.82	4.35	5.62	−4.41	4.89
MG3S CBS10	3.68	−1.61	2.66	3.63	−2.04	2.79
CBSB3 raw				5.18	−4.45	4.53
CBSB3 CBS10				3.02	−2.07	2.42
G3Large raw	4.62	−3.88	3.97	5.07	−4.37	4.42
G3Large CBS10	2.52	−1.23	1.99	2.93	−2.05	2.39
G3XL raw	4.02	−3.34	3.45	4.49	−3.87	3.94
G3XL CBS10	2.29	−0.77	1.82	2.46	−1.61	2.01
G3LargeXP raw	3.93	−3.03	3.26	4.40	−3.61	3.68
G3LargeXP CBS10	2.35	−0.50	1.86	2.59	−1.41	2.14

[a] Error statistics (kcal/mol) refer to the non-MR subset of the W4-08 dataset.

On this issue, it would thus again appear that B2GP-PLYP is a more robust double-hybrid functional than B2K-PLYP.

F. Basis-Set Convergence, Basis-Set Extrapolation, and Inclusion of Inner-Shell Correlation for Double-Hybrid Methods. We have already touched on the issues of basis-set convergence and extrapolation in double-hybrid methods and shown that the aug-pc3+d basis set is quite close to the basis-set limit. This leaves us with the question whether useful results can be obtained with smaller basis sets than this. This is considered in Table 9.

The MG3S combination of Pople basis sets advocated by the Truhlar group clearly is insufficient for double-hybrid functionals, with or without CBS extrapolation. This is perhaps not surprising when all orbitals are correlated, but the issue persists when only valence electrons are correlated. The G3Large basis set employed in G3 theory (which differs from MG3S in a number of high-exponent basis functions) likewise is found wanting without extrapolation but performs tolerably well with CBS extrapolation. The G3XL and G3LargeXP basis sets used in G3X and G4 theory, respectively, work quite well in combination with basis-set extrapolation. The aug-cc-pwCVTZ core-valence basis set is found to be surprisingly close to the basis-set limit, whereas the aug-cc-pwCVQZ basis set, after basis set extrapolation, appears to be of a quality similar to that of aug-pc4.

It is well established that inclusion of inner-shell correlation is essential for high-accuracy ab initio thermochemistry. One would expect its importance to be proportionally smaller for a method that only fractionally relies on ab-initio-style correlation. For the present double-hybrid functionals, we find that although the inclusion of inner-shell correlation does significantly reduce the mean signed error (i.e., overall bias), the improvement in rmsd and MAD is very modest. For most applications, inner-shell correlation can thus be neglected—this is especially useful for systems of heavier elements.

Such neglect has another useful side benefit. Basis-set convergence is noticeably more rapid for the valence-only calculations, and an aug-pc2 + 2d basis set combined with CBS extrapolation is found to get quite close to the basis-set limit. In fact, aug-pc2+2d outperforms both the conventional aug-cc-pV(T+d)Z basis set and the core-valence aug-cc-pwCVTZ basis set, which are computationally somewhat and considerably more expensive, respectively. The B2GP-PLYP/aug-pc2 + 2d/CBS10val combination (where the val suffix denotes that only valence electrons are correlated in the MP2-like step) ought to be sufficient for most practical applications and will run a molecule as large as benzene in under half an hour on 1 CPU using Gaussian 03 with default integration grids.

G. Additional Tests. ***1. Pericyclic Reactions.*** Houk et al.[99,100] presented a test set of 11 pericyclic reactions, for which they analyzed experimental data in detail and also carried out CBS-QB3 calculations. In the BMK paper,[14] W1 calculations were presented for some of these reactions, and in the present work, we are able to compare with W1 data for the first eight of Houk's reactions.

The performance of conventional DFT functionals has been discussed at length elsewhere.[14,99] As for double hybrids, we find here that there is little to choose between them on this criterion because B2T-PLYP, B2GP-PLYP, and B2K-PLYP all yield rms deviations of about 1 kcal/mol.

2. Cumulenes versus Acetylenes. Every conventional DFT functional (with the exception of M06 and M06-2X, as previously noted)[78] that we considered wrongly predicts allene to be more stable than cyclopropene. In contrast, B2GP-PLYP reproduces the W4.2 propyne−allene isomerization energy within +0.2 kcal/mol, whereas B2T-PLYP comes even closer at −0.1 kcal/mol and B2K-PLYP actually overestimates the number by 0.8 kcal/mol. The fact that double-hybrid functionals do not break down for this problem was previously noted by Grimme.[5,88]

3. Rozen's Epoxidation Reaction. The activation barrier for HOF + C_2H_4 → HF + C_2H_4O, a prototype for Rozen's epoxidation reaction,[101,102] is 18.26 kcal/mol at the W1 level.[27] This barrier, which involves a transition state with quite

TABLE 10: Relative Barrier Heights (kcal/mol) for Houk's Hydrocarbon Pericyclic Reaction Set[a]

	W1[b]	CBS-QB3[99]	experiment[99]	experiment[100]	B2GP-PLYP/pc2	B2K-PLYP/pc2
1: cyclobutene → cis-butadiene[b]	35.34[d]	33.7	33.6 ± 0.2	33.6 ± 0.2	35.17	35.88
2: cis-1,3,5-hexatriene → 1,3-cyclohexadiene[c]	30.92	28.8	30.2 ± 0.5	30.2 ± 0.5	29.72	29.74
3: o-xylylene → benzocyclobutene[c]	28.30	25.9	29.8 ± 0.3	28.8 ± 0.3	26.72	26.73
4: cis-1,3-pentadiene sigmatropic shift[b]	39.56	38.9	38.8 ± 0.5	38.8 ± 0.5	35.42	35.73
5: cyclopentadiene sigmatropic shift[b]	28.18	28.1	26.0 ± 0.5	26.0 ± 0.5	27.04	27.03
6: cis-1,5-hexadiene sigmatropic shift[c]	35.64	33.3	34.8 ± 0.5	34.8 ± 0.5	34.55	34.58
7: ethylene + cis-butadiene → cyclohexene[b]	22.14	20.7	21.1 ± 2	22.8 ± 2	21.82	21.33
8: Diels−Alder cyclopentadiene with ethylene[c]	18.26	15.1	19.4 ±21.5	19.5 ± 1.6	17.79	16.97
9: dimerization of cyclopentadiene	N/A	9.8	13.3 ± 0.6	13.3 ± 0.6	14.51	13.26
10:cis-triscyclopropanocyclohexane → 1,4,7-cyclononatriene	N/A	23.5	26.4 ± 3	26.3 ± 3	22.14	22.94
11:cis-triscyclobutanocyclohexane → 1,5,9-cyclododecatriene	N/A	N/A	50.0 ± 3	50.0 ± 3	52.52	54.05

[a] See Figure 1 of ref 99. All values are zero-point exclusive. Differences between experimental values at 0 K and bottom-of-the-well were taken from zero-point corrections found in the Supporting Information of ref 14. Reactions **1**, **4**, **5**, and **7** are taken from the Supporting Information of ref 14. The remaining reactions are from the present work. [b] The SCF and CCSD energies are extrapolated from the cc-pV{T,Q}Z basis set pair, and the CCSD(T) energy from the cc-pV{D,T}Z basis set pair. [c] The SCF and CCSD energies are extrapolated from the aug-cc-pV{T,Q}Z basis set pair on carbon and the cc-pV{T,Q}Z basis set pair on hydrogen and the CCSD(T) energy from the aug-cc-pV{D,T}Z basis set pair on carbon and the cc-pV{D,T}Z basis set pair on hydrogen. [d] For this barrier height, we were able to consider larger basis sets, $\Delta E_e^{\ddagger}$[W2.2] = 35.31 kcal/mol, and post-CCSD(T) contributions, $\Delta E_e^{\ddagger}$[W3.2lite] = 35.10 kcal/mol.

TABLE 11: DFT and W1 Energetics (kcal/mol) for the Prototype Rozen Epoxidation Reaction HOF + C_2H_4 → C_2H_4O + HF

	$\Delta E_e^{\ddagger}$	ΔE_r
B97-1/aug-pc1	8.77	−71.29
B97-1/aug-pc2	13.81	−68.62
B97-1/aug-pc3[a]	14.25	−68.72
B3LYP/aug-pc2	13.68	−66.22
B3PW91/aug-pc2[b]	14.73	−70.90
BMK/aug-pc2	21.79	−73.87
PBE0/aug-pc2	15.47	−73.07
TPSS1KCIS/aug-pc2	14.13	−70.32
B1B95/aug-pc2	17.66	−73.76
BB1K/aug-pc2[b]	24.22	−76.52
mPW1B95/aug-pc2	15.02	−73.26
mPWB1K/aug-pc2[b]	24.24	−77.10
PW6B95/aug-pc2[b]	21.69	−61.47
PWB6K/aug-pc2[b]	28.99	−66.15
TPSS25B95/aug-pc2[b]	15.04	−72.52
TPSS33B95/aug-pc2[b]	18.89	−74.32
M05/aug-pc2[b]	16.83	−84.10
W1	18.26	−71.00
B2-PLYP/aug-pc3	12.36	−70.01
mPW2-PLYP/aug-pc3	14.35	−70.66
B2T-PLYP/aug-pc3	14.84	−71.20
B2GP-PLYP/aug-pc3	15.46	−72.34
B2K-PLYP/aug-pc3	16.82	−73.71
M06L/aug-pc2[b]	8.25 [c]	−72.38
M06/aug-pc2[b]	16.78	−77.69
M06−2X/aug-pc2[b]	25.95	−75.16
M06-HF/aug-pc2[b]	34.87	−73.93

[a] Single-point calculation at B97-1/aug-pc2 geometry. [b] Single-point calculation at B1B95/aug-pc2 geometry. [c] The 0.25 value reported in ref 1 is a typo.

unorthodox HO^+ and F^- moieties, is quite a difficult test for DFT functionals.[27] Results are gathered in Tables 10 and 11. The W1 reference values are 18.3 kcal/mol for the barrier and −71.0 for the reaction energy. With the aug-pc3 basis set, B2-PLYP, mPW2-PLYP, and B2T-PLTP yield significantly underestimated barriers of 12.4, 14.4, and 14.8 kcal/mol, respectively, whereas B2K-PLYP reaches a respectable 16.8 kcal/mol. However, B2K-PLYP clearly overestimates the overall exothermicity, whereas B2T-PLYP reproduces it almost exactly and B2-PLYP underestimates it by 1 kcal/mol. B2GP-PLYP is in a compromise position, with a barrier of 15.5 kcal/mol and a reaction energy of −72.3 kcal/mol.

Out of the conventional functionals, B1B95 (perhaps fortuitously) puts in the best performance overall. We note that the M06 functional yields an excellent barrier, 16.8 kcal/mol, but the reaction exothermicity is grossly overestimated. The other members of the family are seriously wrong: the calculated barriers are 8.3, 26.0, and 34.9 kcal/mol for M06L, M06−2X, and M06-HF, respectively. M06L, and to a lesser extent M06-HF, reproduce the exothermicity fairly well.

4. Dispersion-Driven Isomerization Energies: n-Octane versus Hexamethylethane. Grimme[109] noted that almost all DFT functionals predict the wrong sign for the isomerization energy from *n*-octane, $CH_3(CH_2)_6CH_3$, to hexamethylethane (a.k.a., 2,2,3,3-tetramethylbutane), $(CH_3)_3CC(CH_3)_3$, or tBu-tBu. Naively, on grounds of steric crowding, one would expect *n*-octane to have the more stable structure, and as can be seen in Table 12, this is indeed the case at the Hartree−Fock level. However, dispersion strongly favors the fully branched structure, and the experimental $\Delta H^{\circ}_{r,0}$ for the reaction is −1.9 ± 0.5 kcal/mol.

We attempted to calculate the energy difference ab initio at the valence-only W1h level from B3LYP/pc-2 reference geometries. An idealized structure for tBu-tBu would have D_{3d} symmetry; at all levels of theory that we considered, this structure is a first-order saddle point, and a mild torsion along the tBu-tBu axis leads to a global minimum with D_3 symmetry. The deformation energy is found to be an essentially constant −0.45 kcal/mol at levels of theory ranging from HF/cc-pVDZ to CCSD(T)/aug-cc-pVTZ.

Because the largest nondegenerate subgroup of D_3 is only C_2, CCSD/cc-pVQZ or CCSD/aug′-cc-pVQZ calculations, as required for W1h and W1, respectively, were beyond the disk space and memory limitations of our available hardware. However, we were able to do a W1h calculation on the energy difference between C_{2h} *n*-octane and the D_{3d} saddle point and obtained −1.01 kcal/mol. (We note in passing that the basis-set limit SCF, CCSD correlation, and (T) components of this number are +11.46, −10.31, and −2.16 kcal/mol, respectively, illustrating the very high importance of correlation for this equilibrium.) Combined with the deformation energy of −0.45 kcal/mol, this leads to $\Delta H_{r,e}$ = −1.46 kcal/mol.

TABLE 12: Reaction Energies for CH_3 -$(CH_2)_6$-CH_3 → $(tBu)_2$ (kcal/mol, Nonrelativistic, Clamped Nuclei)

method	energy
experiment[109]	−1.9 ± 0.5
W1h	−1.5
B2GP-PLYP raw	+1.96
ditto CBS10val	+1.81
B2K-PLYP raw	+1.18
M06	−1.91
M06-2X	−1.13
HF	+10.63
MP2	−4.32
SCS-MP2	−1.34
B2-PLYP	+3.27
B2-PLYP+D	−2.31 [$s_6 = 0.55$]
mPW2-PLYP	+2.87
mPW2-PLYP CBS10	+2.77
mPW2+PLYP+D	−1.19 [$s_6 = 0.40$]
B3LYP	+7.96
B3LYP+D	−2.70 [$s_6 = 1.05$]
PBE0	+5.08
PBE0+D	−2.03 [$s_6 = 0.70$]
B97-1	+5.83
BMK	+1.93
BMK+D	−4.67 [$s_6 = 0.65$]
B2GP-PLYP+D	−2.10 [$s_6 = 0.40$]
B2K-PLYP+D	−1.87 [$s_6 = 0.30$]

[a] The pc-2 basis set was used throughout. The unscaled Grimme dispersion correction ($s_6 = 1.0$) amounts to −10.15 kcal/mol for this reaction.

We already noted that HF is grossly biased toward *n*-octane. MP2 overcorrects at −4.32 kcal/mol, whereas SCS-MP2[110] reproduces the reference value almost exactly. The M06 and M06-2X functionals bracket the correct number, whereas older-generation DFT functionals such as (in decreasing order of error) B3LYP, PBE0, B97−1, and even BMK all yield the wrong sign. The error is mitigated in the double hybrids, decreasing (as expected) with increasing percentage of MP2 correlation. Yet, this problem illustrates once again that even double hybrids need a little help for phenomena that are largely dispersion-driven. Introducing Grimme's Lennard-Jones-type dispersion correction results in a qualitatively correct answer even for B3LYP, while PBE0+D actually gets quite close to the right answer. The B2x-PLYP+D family yields answers near −2 kcal/mol as well, whereas mPW2-PLYP+D slightly errs on the opposite side of the reference value.

5. Benzene Dimer Structures. Benzene dimer is probably the most studied prototype π-stacking system; theoretical and experimental work has been reviewed by Sinnokrot and Sherrill.[111]

Very recently, Janowski and Pulay[112] carried out benchmark ab initio calculations at levels as high as QCISD(T)/AVTZ for the whole potential energy surface and QCISD(T)/AVQZ for the dissociation energies at the stationary points. The latter are among the largest-scale coupled cluster calculations performed to date.

The D_{6h} stacked structure is a first-order saddle point, corresponding to the transition state for a ring slippage connecting two equivalent parallel-displaced C_{2h} structures. A C_{2v} T-shaped structure with one benzene ring standing at a 90° angle above the other (one hydrogen above the center of the other ring) constitutes the other principal minimum structure. Both benchmark studies find the slipped and T-shaped structures to be nearly isoenergetic; Sinnokrot and Sherrill find the slipped structure to be marginally more stable, whereas Janowski and Pulay (JP) find the opposite. In both cases, the difference can be considered to be within the computational uncertainty.

TABLE 13: Dissociation Energies (kcal/mol) for C_{2h} Slipped (i.e., Parallel-Displaced), D_{6h} Stacked, and C_{2v} T-Shaped Structures of Benzene Dimer[a]

method	slipped	T-shaped	stacked
Sinnokrot and Sherrill[111]	2.78	2.74	1.81
QCISD(T)/AV ∞ Z[112]	2.521(2.659)	2.524(2.683)	1.576(1.653)
SCS-MP2/AV ∞ Z[112]	2.874(2.855)	2.452(2.468)	1.898(1.858)
MP2/AV ∞ Z[112]	4.535(4.534)	3.475(3.510)	3.155(3.132)
CCSD(T)/AVTZ[112]	(2.546)	(2.569)	(1.598)
QCISD(T)/AVTZ[112]	3.813(2.550)	3.773(2.573)	2.532(1.602)
B3LYP/apc2	−2.37	−0.54	−2.30
ditto+D	2.08	2.87	1.33
M06/apc2	1.64	1.44	0.42
M06-2X/apc2	2.01	2.21	0.37
PBE0/apc2	−0.86	0.65	−1.19
ditto+D	2.11	2.92	1.23
BMK/apc2	−1.03	−0.01	−2.10
B97-1/apc2	−0.38	0.81	−0.64
B2GP-PLYP/apc2	1.79(0.56)	2.36(1.30)	0.87(−0.05)
ditto+D	3.49(2.26)	3.65(2.59)	2.26(1.34)
B2-PLYP/apc2	0.81(−0.16)	1.65(0.92)	0.15(−0.69)
ditto+D	3.14(2.17)	3.43(2.70)	2.05(1.31)
B2T-PLYP/apc2	1.28(0.19)	2.01(1.19)	0.48(−0.49)
B2K-PLYP/apc2	2.38(0.98)	2.79(1.74)	1.31(0.11)
ditto+D	3.65(2.25)	3.76(2.71)	2.34(1.15)
mPW2-PLYP/apc2	1.32(0.42)	2.11(1.43)	0.56(−0.22)
ditto+D	3.02(2.12)	3.40(2.72)	1.95(1.17)

[a] Values enclosed in parentheses include the Boys−Bernardi counterpoise correction. All calculations on these structures in the present work were performed at the QCISD(T)/AVTZ optimized geometries of Janowski and Pulay.[112]

In the present work (Table 13), we find that popular DFT functionals generally predict the T-shaped structure to be much more stable than the others and that functionals such as B3LYP even fail to produce positive binding energies for any of the structures. M06, on the other hand, reproduces the relative energies of the three structures very well, even though it consistently underbinds all three.

Dispersion is rather important for this interaction, as illustrated by the shrill contrast between the poor performance of B3LYP or PBE0 and the quite reasonable results obtained for both functionals with Grimme's dispersion correction. As noted by JP, MP2 seriously overbinds all three structures and is biased toward the stacked and ring-slipped structures. B2GP-PLYP does not seem to suffer from these particular defects, although it somewhat underbinds all three structures. Adding a dispersion correction leads to mild overbinding; additionally including counterpoise corrections leads to mild underbinding. This suggests that B2GP-PLYP+D would be very close to the benchmark values at the basis-set limit.

V. Conclusions

In the first part of the paper, we have presented sub-kJ/mol accuracy reference data for about 100 total atomization energies of molecules and radicals (the W4-08 data set) and for the DBH24 set of representative barrier heights from the Truhlar group. In addition, we obtained benchmark quality ab initio reference data for several ancillary DFT torture tests, such as the isomers of C_3H_4, the *n*-octane−hexamethylethane equilibrium, Houk's pericyclic reactions, and more.

In the second part of the paper, we have employed these data for the parametrization and validation of double-hybrid density functionals, primarily those employing mixtures of Becke GGA and Hartree−Fock-type exchange on the one hand, and LYP GGA and MP2-type correlation on the other hand. We have arrived at the following conclusions:

• On the B2x-PLYP surface, quite different double hybrids are optimum for different reaction barrier types: (39,71) for Hxfers, (61,82) for SN2s, (35,57) for UAR reactions, and (28,62) for HATs.

• Because the basin for the HATs is the steepest, the optimum for the DBH24-W4 barrier set is (30,64).

• Recalling our earlier observation[1] that thermochemistry for the W3 set is basically optimum along a very narrow strait with its minimum at (31,60), we obtain an optimum of (42,72) for the average of Hxfer barrier heights and the W3 thermochemistry set, which we earlier denoted[1] B2K-PLYP.

• For the average of DBH24-W4 kinetics and W3 thermochemistry data, (36,65) is the optimum, which we here denote B2GP-PLYP.

• Although B2K-PLYP yields excellent Hxfer barriers and outstanding SN2 barriers, B2GP-PLYP is superior for these latter two reaction types and overall has the more balanced performance for the different reaction types.

• Although both B2K-PLYP and B2GP-PLYP yield excellent thermochemical performance (rmsds of about 2 kcal/mol, comparable to G2 and G3 theory for the data set tested), B2GP-PLYP appears to be the more robust of the two toward nondynamical correlation and strongly polar bonding.

• All double hybrids perform excellently for pericyclic reaction barriers (rmsd of about 1 kcal/mol).

• B2K-PLYP and especially B2GP-PLYP yield excellent performance for barrier heights of prototype late transition metal insertion reactions, unlike kinetics-friendly hybrid meta-GGAs such as BMK and M06(−2X).

• B2K-PLYP and B2GP-PLYP also pass several other difficult tests of DFT methods, such as the relative energies of C_3H_4 isomers.

• All double hybrids, including B2GP-PLYP, yield excellent performance for hydrogen bonds, whereas more dispersion-driven weak interactions (such as in benzene dimer, as well as those governing the *n*-octane-tetramethylbutane equilibrium) still require empirical dispersion corrections.

• In general, we recommend B2GP-PLYP as a reliable general-purpose method, with B2K-PLYP retained for scenarios where performance for Hxfer and/or SN2 barriers is paramount.

• Confirming earlier observations by Grimme, similar quality double hybrids can be obtained with several other exchange functionals, but the LYP correlation functional appears to be critical for this level of performance. A tentative argument why is offered.

• Empirical dispersion correction coefficients for the new double hybrids, as well as for a number of traditional DFT functionals such as B3PW91, PBE0, BMK, and the M06 family, have been derived and presented.

We would like to emphasize that B2GP-PLYP, as B2K-PLYP, can be run by using unmodified copies of such quantum chemical codes as Gaussian 03[103] and ORCA.[104]

Acknowledgment. Research at Weizmann was funded by the Israel Science Foundation (Grant no. 709/05), the Minerva Foundation (Munich, Germany), the Helen and Martin Kimmel Center for Molecular Design (Weizmann), and the Weizmann Institute Alternative Energy Research Initiative (AERI). Research at Northwestern was funded by the Air Force Office of Scientific Research (Grant no. FA9550-07-1-0095). G.C.S. is a Charles E. and Emma H. Morrison Professor of Chemistry. J.M.L.M. is the incumbent of the Baroness Thatcher Professorial Chair of Chemistry as well as a member ad personam of the Lise Meitner-Minerva Center for Computational Quantum Chemistry. The authors would like to thank Dr. Mark A. Iron and Dr. A. Daniel Boese for helpful discussions and Prof. George A. Petersson (Wesleyan U.) for useful suggestions concerning the CBS extrapolation.

Supporting Information Available: Tables S-1 and S-2; complete reference for Gaussian 03; component breakdown and multireference character diagnostics for the W4-08 and DBH24 sets; reference geometries for the W4-08 and DBH24 sets; references for zero-point vibrational energies in W4.08 set. This material is available free of charge via the Internet at http://pubs.acs.org.

Note Added in Proof. Two larger hydrogen-bonded species in the HB6 set of Zhao and Truhlar,[80] namely, formamide dimer and formic acid dimer, were not included in the W2-level study of Boese et al.[70] Our W2 results for the equilibrium dimerization energies of formamide and formic acid are 14.93 and 16.22 kcal/mol, respectively, which differ insignificantly from the W1 values of Zhao and Truhlar.

References and Notes

(1) Tarnopolsky, A.; Karton, A.; Sertchook, R.; Vuzman, D.; Martin, J. M. L. *J. Phys. Chem. A* **2008**, *112*, 3.

(2) Raghavachari, K.; Curtiss, L. A. In *Quantum-Mechanical Prediction of Thermochemical Data*; Cioslowski, J., Ed.; Kluwer: Dordrecht, 2001.

(3) Petersson, G. A. In *Quantum-Mechanical Prediction of Thermochemical Data*; Cioslowski, J., Ed.; Kluwer: Dordrecht, 2001.

(4) (a) Zhao, Y.; Lynch, B. J.; Truhlar, D. G. *J. Phys. Chem. A* **2004**, *108*, 4786. (b) Zhao, Y.; Lynch, B. J.; Truhlar, D. G. *Phys. Chem. Chem. Phys.* **2005**, *7*, 43.

(5) Grimme, S. *J. Chem. Phys.* **2006**, *124*, 034108.

(6) Schwabe, T.; Grimme, S. *Phys. Chem. Chem. Phys.* **2006**, *8*, 4398.

(7) Perdew, J. P.; Schmidt, K. In *Density Functional Theory and its Application to Materials*; Van Doren, V., Van Alsenoy, C., Geerlings, P., Eds.; AIP Conference Proceedings, **2001**; *577*, 1.

(8) Becke, A. D. *Phys. Rev. A* **1988**, *38*, 3098.

(9) Lee, C.; Yang, W.; Parr, R. G. *Phys. Rev. B* **1988**, *37*, 785.

(10) (a) Perdew, J. P.; Burke, K.; Ernzerhof, M. *Phys. Rev. Lett.* **1996**, *77*, 3865. (b) Erratum: **1997**, *78*, 1396.

(11) Adamo, C.; Barone, V. *J. Chem. Phys.* **1999**, *110*, 6158.

(12) (a) PW91 exchange functional Perdew, J. P.; Wang, Y. *Phys. Rev. B* **1992**, *45*, 13244. (b) PW91 correlation functional Perdew, J. P.; Chevary, J. A.; Vosko, S. H.; Jackson, K. A.; Pederson, M. R.; Singh, D. J.; Fiolhais, C. *Phys. Rev. B* **1992**, *46*, 6671.

(13) (a) Becke, A. D. *J. Chem. Phys.* **1993**, *98*, 5648. (b) Note that the actual correlation functional considered for use with the 3-parameter hybrid exchange proposed in what is popularly cited as the B3LYP paper is actually PW91.[12] The paper that first suggested replacement of PW91 with LYP is Stephens, P. J.; Devlin, F. J.; Chabalowski, C. F.; Frisch, M. J. *J. Phys. Chem.* **1994**, *98*, 11623–11627.

(14) Boese, A. D.; Martin, J. M. L. *J. Chem. Phys.* **2004**, *121*, 3405.

(15) Zhao, Y.; Truhlar, D. G. *J. Chem. Phys.* **2006**, *125*, 194101.

(16) Zhao, Y.; Truhlar, D. G. *J. Phys. Chem. A* **2006**, *110*, 13126.

(17) (a) Zhao, Y.; Truhlar, D. G. *Theor. Chem. Acc.* **2008**, *120*, 215. (b) Erratum: **2008**, *119*, 525.

(18) Zhao, Y.; Truhlar, D. G. *Acc. Chem. Res.* **2008**, *41*, 157.

(19) Kümmel, S.; Kronik, L. *Rev. Mod. Phys.* **2008**, *80*, 3.

(20) Görling, A.; Levy, M. *Phys. Rev. B* **2007**, *47*, 13105.

(21) Adamo, C.; Barone, V. *J. Chem. Phys.* **1998**, *108*, 664.

(22) Frisch, M. J.; Trucks, G. W.; Schlegel, H. B.; Scuseria, G. E.; Robb, M. A.; Cheeseman, J. R.; Montgomery, J. A., Jr.; Vreven, T.; Kudin, K. N.; Burant, J. C.; Millam, J. M.; Iyengar, S. S.; Tomasi, J.; Barone, V.; Mennucci, B.; Cossi, M.; Scalmani, G.; Rega, N.; Petersson, G. A.; Nakatsuji, H.; Hada, M.; Ehara, M.; Toyota, K.; Fukuda, R.; Hasegawa, J.; Ishida, M.; Nakajima, T.; Honda, Y.; Kitao, O.; Nakai, H.; Klene, M.; Li, X.; Knox, J. E.; Hratchian, H. P.; Cross, J. B.; Bakken, V.; Adamo, C.; Jaramillo, J.; Gomperts, R.; Stratmann, R. E.; Yazyev, O.; Austin, A. J.; Cammi, R.; Pomelli, C.; Ochterski, J. W.; Ayala, P. Y.; Morokuma, K.; Voth, G. A.; Salvador, P.; Dannenberg, J. J.; Zakrzewski, V. G.; Dapprich, S.; Daniels, A. D.; Strain, M. C.; Farkas, O.; Malick, D. K.; Rabuck, A. D.; Raghavachari, K.; Foresman, J. B.; Ortiz, J. V.; Cui, Q.; Baboul, A. G.; Clifford, S.; Cioslowski, J.; Stefanov, B. B.; Liu, G.; Liashenko, A.; Piskorz, P.; Komaromi, I.; Martin, R. L.; Fox, D. J.; Keith, T.; Al-Laham, M. A.; Peng, C. Y.; Nanayakkara, A.; Challacombe, M.; Gill, P. M. W.; Johnson, B.; Chen, W.; Wong, M. W.; Gonzalez, C.; Pople, J. A. *Gaussian 03*, revision C.01; Gaussian, Inc.: Wallingford, CT, 2004.

(23) Neese, F.; Schwabe, T.; Grimme, S. *J. Chem. Phys.* **2007**, *126*, 124115.

(24) ORCA is an electronic structure program package written by Neese, F. with contributions from Becker, U.; Ganiouchine, D.; Kossmann, S. Petrenko; T. Riplinger, C.; Wennmohs, F. See also http://www.thch.uni-bonn.de/tc/orca.

(25) For a brief review of the Resolution of the Identity (RI) approach, see Kendall, R. A.; Früchtl, H. A. *Chem. Acc.* **1997**, *97*, 158.

(26) Neese, F. Outstanding Young German Scientist lecture. *Lise Meitner-Minerva Center for Computational Quantum Chemistry*; Hebrew University of Jerusalem: Israel, June 19, 2007).

(27) Sertchook, R.; Boese, A. D.; Martin, J. M. L. *J. Phys. Chem. A* **2006**, *110*, 8275.

(28) Sundermann, A.; Uzan, O.; Milstein, D.; Martin, J. M. L. *J. Am. Chem. Soc.* **2000**, *122*, 7095.

(29) Sundermann, A.; Uzan, O.; Martin, J. M. L. *Organometallics* **2001**, *20*, 1783.

(30) Rybtchinski, B.; Oevers, S.; Montag, M.; Vigalok, A.; Rozenberg, H.; Martin, J. M. L.; Milstein, D. *J. Am. Chem. Soc.* **2001**, *123*, 9064.

(31) Iron, M. A.; Sundermann, A.; Martin, J. M. L. *J. Am. Chem. Soc.* **2003**, *125*, 11430.

(32) Brunsvold, A. L.; Zhang, J.; Upadhyaya, H. P.; Minton, T. K.; Camden, J. P.; Paci, J. T.; Schatz, G. C. *J. Phys. Chem. A.* **2007**, *111*, 10907.

(33) Camden, J. P.; Schatz, G. C. *J. Phys. Chem. A.* **2006**, *110*, 13681–13685.

(34) Quintal, M. M.; Karton, A.; Iron, M. A.; Boese, A. D.; Martin, J. M. L. *J.Phys. Chem. A* **2006**, *110*, 709.

(35) Martin, J. M. L.; Oliveira, G. *J. Chem. Phys.* **1999**, *111*, 1843.

(36) Parthiban, S.; Martin, J. M. L. *J. Chem. Phys.* **2001**, *114*, 6014.

(37) Boese, A. D.; Oren, M.; Atasoylu, O.; Martin, J. M. L.; Kállay, M.; Gauss, J. *J. Chem. Phys.* **2004**, *120*, 4129.

(38) Karton, A.; Rabinovich, E.; Martin, J. M. L.; Ruscic, B. *J. Chem. Phys.* **2006**, *125*, 144108.

(39) Karton, A.; Ruscic, B.; Martin, J. M. L. *J. Mol. Struct. (Theochem)* **2007**, *811*, 345–353.

(40) Karton, A.; Taylor, P. R.; Martin, J. M. L. *J. Chem. Phys.* **2007**, *127*, 064104.

(41) Karton, A.; Martin, J. M. L. *J. Phys. Chem. A* **2007**, *111*, 5936–5944.

(42) Karton, A.; Martin, J. M. L. *Mol. Phys.* **2007**, *105*, 2499.

(43) MRCC, a string-based general coupled cluster program suite written by Kállay, M.; Kállay, M.; Surján, P. R. *J. Chem. Phys.* **2001**, *115*, 2945.

(44) ACES II (Austin−Mainz−Budapest version) is an electronic structure program system written by Stanton, J. F.; Gauss, J.; Watts, J. D.; Szalay, P. G.; Bartlett, R. J. with contributions from Auer, A. A.; Bernholdt, D. B.; Christiansen, O.; Harding, M. E.; Heckert, M.; Heun, O.; Huber, C.; Jonsson, D.; Jusélius, J.; Lauderdale, W. J.; Metzroth, T.; Ruud, K.

(45) MOLPRO is a package of ab initio programs written by Werner, H.-J.; Knowles, P. J.; Schütz, M.; Lindh, R.; Celani, P.; Korona, T.; Rauhut, G.; Manby, F. R.; Amos, R. D.; Bernhardsson, A.; Berning, A.; Cooper, D. L.; Deegan, S.; Dobbyn, M. J. O.; Eckert, A. J.; Hampel, F.; Hetzer, C.; Lloyd, G.; McNicholas, A. W. J.; Meyer, W.; Mura, M. E.; Nicklaβ, A.; Palmieri, P.; Pitzer, R.; Schumann, U.; Stoll, H.; Stone, A. J.; Tarroni, R.; Thorsteinsson, T.

(46) Wood, G. P. F.; Radom, L.; Petersson, G. A.; Barnes, E. C.; Frisch, M. J.; Montgomery, J. A. *J. Chem. Phys.* **2007**, *125*, 094106 and references therein.

(47) Curtiss, L. A.; Raghavachari, K.; Trucks, G. W.; Pople, J. A. *J. Chem. Phys.* **1991**, *94*, 7221.

(48) Curtiss, L. A.; Raghavachari, K.; Redfern, P. C.; Rassolov, V.; Pople, J. A. *J. Chem. Phys.* **1998**, *109*, 7764.

(49) Montgomery, J. A., Jr.; Frisch, M. J.; Ochterski, J. W.; Petersson, J. G. A. *Chem. Phys.* **1999**, *110*, 2822, and references therein.

(50) Curtiss, L. A.; Redfern, P. C.; Raghavachari, K.; Pople, J. A. *J. Chem. Phys.* **2001**, *114*, 108.

(51) Curtiss, L. A.; Redfern, P. C.; Raghavachari, K. *J. Chem. Phys.* **2007**, *126*, 084108 and references therein.

(52) (a) Jensen, F. *J. Chem. Phys.* **2001**, *115*, 9113. (b) Erratum: 2002, *116*, 3502.

(53) Jensen, F. *J. Chem. Phys.* **2002**, *116*, 7372.

(54) Jensen, F. *J. Chem. Phys.* **2002**, *117*, 9234.

(55) Jensen, F.; Helgaker, T. *J. Chem. Phys.* **2004**, *121*, 3463.

(56) Jensen, F. *J. Phys. Chem. A* **2007**, *111*, 11198.

(57) Martin, J. M. L. *J. Mol. Struct. (Theochem)* **2006**, *771*, 19, and references therein.

(58) Becke, A. D. *J. Chem. Phys.* **1996**, *104*, 1040.

(59) (a) Becke, A. D. *J. Chem. Phys.* **1997**, *107*, 8554. (b) Hamprecht, F.; Cohen, A. J.; Tozer, D. J.; Handy, N. C. *J. Chem. Phys.* **1998**, *109*, 6264.

(60) Tao, J. M.; Perdew, J. P.; Staroverov, V. N.; Scuseria, G. E. *Phys. Rev. Lett.* **2003**, *91*, 146401.

(61) Krieger, J. B.; Chen, J.; Iafrate, G. J.; Savin, A. Construction of an accurate self-interaction-corrected correlation energy functional based on an electron gas with a gap. In *Electron Correlations and Materials Properties*; Gonis, A., Kioussis, N., Eds.; Plenum: New York, 1999.

(62) Zhao, Y.; Lynch, B. J.; Truhlar, D. G. *Phys. Chem. Chem. Phys.* **2005**, *7*, 43–52.

(63) Zhao, Y.; Lynch, B. J.; Truhlar, D. G. *J. Phys. Chem. A* **2004**, *108*, 2715.

(64) Zhao, Y.; Truhlar, D. G. *J. Phys. Chem. A* **2004**, *108*, 6908.

(65) Zhao, Y.; Truhlar, D. G. *J. Phys. Chem. A* **2005**, *109*, 5656.

(66) (a) Ruscic, B.; Pinzon, R. E.; Morton, M. L.; von Laszewski, G.; Bittner, S.; Nijsure, S. G.; Amin, K. A.; Minkoff, M.; Wagner, A. F. *J. Phys. Chem. A* **2004**, *108*, 9979–9997. (b) Ruscic, B.; Pinzon, R. E.; von Laszewski, G.; Kodeboyina, D.; Burcat, A.; Leahy, D.; Montoya, D.; Wagner, A. F. Active Thermochemical Tables: Thermochemistry for the 21st Century. *J. Phys. Conf. Ser.* **2005**, *16*, 561–570.

(67) Zheng, J.; Zhao, Y.; Truhlar, D G. *J. Chem. Theory Comput.* **2007**, *3*, 569. Note that some of the geometries in the Supporting Information of this paper exhibit very small deviations from proper symmetry. Because an extra symmetry element can easily make the difference between a feasible and an unfeasible W4 or W3.2 calculation, we have symmetrized such geometries and reoptimized them at the original QCISD/MG3 level of theory. In all such cases, the optimizations converged in one or two cycles.

(68) Pople, J. A.; Head-Gordon, M.; Raghavachari, K. *J. Chem. Phys.* **1987**, *87*, 5968.

(69) Zhao, Y.; González-García, N.; Truhlar, D. G. *J. Phys. Chem. A* **2005**, *109*, 2012(erratum **2006**, *110*, 4942)

(70) Boese, A. D.; Martin, J. M. L.; Klopper, W. *J. Phys. Chem. A.* **2007**, *111*, 11122.

(71) Ruscic, B.; Boggs, J. E.; Burcat, A.; Csaszar, A. G.; Demaison, J.; Janoschek, R.; Martin, J. M. L.; Morton, M. L.; Rossi, M. J.; Stanton, J. F.; Szalay, P. G.; Westmoreland, P. R.; Zabel, F.; Berces, T. IUPAC Critical Evaluation of Thermochemical Properties of Selected Radicals. Part I. *J. Phys. Chem. Ref. Data* **2005**, *34*, 573–656. See also http://www.iupac.org/web/ins/2003-024-1-100.

(72) Martin, J. M. L. *J. Chem. Phys.* **1998**, *108*, 2791.

(73) (a) Martin, J. M. L. *Chem. Phys. Lett.* **1999**, *310*, 271–276. (b) Martin, J. M. L. *Spectrochimica Acta A* **1999**, *55*, 709–718.

(74) Karton, A.; Parthiban, S.; Martin, J. M. L. in preparation.

(75) (a) Kraka, E.; He, Y.; Cremer, D. *J. Phys. Chem. A* **2001**, *105*, 3269–3276. (b) Feller, D.; Dixon, D. A. *J. Phys. Chem. A* **2003**, *107*, 9641–9651. (c) Lee, T. J.; Rice, J. E.; Dateo, C. E. *Mol. Phys.* **1996**, *89*, 1359–1372. (d) Ellingson, B. A.; Theis, D. P.; Tishchenko, O.; Zheng, J.; Truhlar, D. G. *J. Phys. Chem. A* **2007**, *111*, 13554.

(76) Johnson, R. D., Ed. *NIST Computational Chemistry Comparison and Benchmark Database*, Release 12 (August 2005). http://srdata.nist.gov/cccbdb.

(77) Woodcock, H. L.; Schaefer, H. F.; Schreiner, P. R. *J. Phys. Chem. A* **2002**, *106*, 11923.

(78) Zhao, Y.; Truhlar, D. G. *J. Phys. Chem. A* **2006**, *110*, 10478.

(79) Colle, R.; Salvetti, O. *Theor. Chim. Acta* **1975**, *37*, 329.

(80) Zhao, Y.; Truhlar, D. G. *J. Chem. Theor. Comput.* **2005**, *1*, 415.

(81) Jurecka, P.; Sponer, J.; Cerny, J.; Hobza, P. *Phys. Chem. Chem. Phys.* **2006**, *8*, 1985.

(82) Zhang, Y.; Li, Z. H.; Truhlar, D. G. *J. Chem. Theor. Comput.* **2007**, *3*, 289.

(83) (a) Allen, M. J.; Tozer, D. J. *J. Chem. Phys.* **2002**, *117*, 11113. (b) Tsuzuki, S.; Lüthi, H.-P. *J. Chem. Phys.* **2001**, *114*, 3949. (c) For an alternative approach based on pure Hartree−Fock exchange, see Becke, A. D.; Johnson, E. R. *J. Chem. Phys.* **2007**, *127*, 154108, and references therein.

(84) Zimmerli, U.; Parrinello, M.; Koumoutsakos, P. *J. Chem. Phys.* **2004**, *120*, 2603.

(85) Wu, Q.; Yang, W. *J. Chem. Phys.* **2002**, *116*, 515.

(86) Grimme, S. *J. Comput. Chem.* **2004**, *25*, 1463.

(87) Grimme, S. *J. Comput. Chem.* **2006**, *27*, 1787. The dispersion coefficient, radii, and hysteresis exponent ($\alpha = 20$) from the latter paper were used throughout whenever a +D correction is considered in the present work.

(88) Schwabe, T.; Grimme, S. *Phys. Chem. Chem. Phys.* **2007**, *9*, 3397.

(89) Schäfer, A.; Huber, C.; Ahlrichs, R. *J. Chem. Phys.* **1994**, *100*, 5829.

(90) Boys, S. F.; Bernardi, F. *Mol. Phys.* **1970**, *19*, 553.

(91) Halkier, A.; Koch, H.; Jørgensen, P.; Christiansen, O.; Beck Nielsen, I. M.; Helgaker, T. *Theor. Chem. Acc.* **1997**, *97*, 150–157.

(92) Xu, X.; Goddard, W. A. *Proc. Nat. Acad. Sci. U.S.A.* **2004**, *101*, 2673.

(93) Schultz, N. E.; Zhao, Y.; Truhlar, D. G. *J. Comput. Chem.* **2008**, *29*, 185.

(94) (a) Nyden, M. R.; Petersson, G. A. *J. Chem. Phys.* **1981**, *75*, 1843. (b) Petersson, G. A.; Al-Laham, M. A. *J. Chem. Phys.* **1991**, *94*, 6081.

(95) (a) Petersson, G. A.; Tensfeldt, T.; Montgomery, J. A. *J. Chem. Phys.* **1991**, *94*, 6091. (b) Montgomery, J. A.; Ochterski, J. W.; Petersson,

G. A. *J. Chem. Phys.* **1994**, *101*, 5900. (c) Petersson, G. A. Personal communication.

(96) (a) Cioslowski, J.; Mixon, S. T. *Inorg. Chem.* **1993**, *32*, 3209. (b) Reed, A. E.; von Ragué Schleyer, R. *J. Am. Chem. Soc.* **1990**, *112*, 1434.

(97) Bauschlicher, C. W., Jr.; Partridge, H. *Chem. Phys. Lett.* **1995**, *240*, 533.

(98) Wilson, A. K.; Peterson, K. A.; Dunning, T. H., Jr *J. Chem. Phys.* **2001**, *114*, 9244.

(99) Guner, V.; Khuong, K. S.; Leach, A. G.; Lee, P. S.; Bartberger, M. D.; Houk, K. N. *J. Chem. Phys. A* **2003**, *107*, 11445.

(100) Ess, D. H.; Houk, K. N. *J. Phys. Chem. A* **2005**, *109*, 9542.

(101) Rozen, S. *Acc. Chem. Res.* **1996**, *29*, 243–248.

(102) Rozen, S. *Pure Appl. Chem.* **1999**, *71*, 481–487.

(103) The following nonstandard Gaussian 03 route will do the required steps for a B2GP-PLYP calculation: #P blyp/Gen IOp(3/76=0350006500,3/78=0640006400) extraoverlay scf=tight [blank line] 8/10=90/1; 9/16=−3/6; [blank line, followed by rest of input]. In order to carry out a CBS extrapolation on the MP2 energy, replace the last line by 8/10=90/1; 9/16=−3,75=2,81=Nmin/6,4;, where Prof. Petersson recommends setting the pair extrapolation parameter N_{min} to 5 for an spd basis set, 10 for an spdf basis set, and so forth. In order to freeze inner-shell electrons, replace "8/10=90" by "8/10=2.

(104) The following nonstandard ORCA input will do the required steps for a B2GP-PLYP calculation:

```
% method
  exchange X_B88
  correlation C_LYP
  ldaopt C_VWN3
  ScalHFX = 0.65
  ScalDFX = 0.35
  ScalMP2c = 0.36
  ScalLDAc = 0.64
  ScalGGAc = 0.64
end.
```

(105) Peterson, K. A.; Dunning, T. H. *J. Chem. Phys.* **2002**, *117*, 10548.

(106) (a) Stone, A. J. *The theory of intermolecular forces*; Clarendon Press: Oxford, 1996. (b) Stone, A. J. *Chem. Phys. Lett.* **1993**, *211*, 101.

(107) Davidson, E. R. *Int. J. Quantum Chem.* **2004**, *98*, 317.

(108) Wenthold, P. G.; Squires, R. R. *J. Phys. Chem.* **1995**, *99*, 2002.

(109) Grimme, S. *Angew. Chem., Int. Ed.* **2006**, *45*, 4460.

(110) Grimme, S. *Angew. Chem., Int. Ed.* **2003**, *118*, 9095.

(111) Sinnokrot, M. O.; Sherrill, C. D. *J. Phys. Chem. A* **2006**, *110*, 10656–10668.

(112) Janowski, T.; Pulay, P. *Chem. Phys. Lett.* **2007**, *447*, 27–32.

JP801805P